國 立 交 通 大 學
生物科技研究所
碩 士 論 文

克雷白氏肺炎桿菌 CG43 莢膜多醣體的產生和酪胺酸磷酸化作用的研究

Capsular polysaccharide production and protein-tyrosine phosphorylation in *Klebsiella pneumoniae* CG43

研 究 生：白平輝
學　　號：9128526
指導教授：彭慧玲 博士

中華民國九十三年七月

致謝

雖然我是生物背景，但是上研究所之前，除了實驗課之外，沒有真正接觸過實驗，這一篇論文的完成，真的要感謝很多人的幫忙。最感謝彭老師給我機會進入生科所，又讓我進入實驗室，除了提供好的環境、研究材料，更在實驗上給我許多建議和幫助；尤其，我是一個有點不專注、鬆散的人，老師讓我體會到一位好的研究者該有的嚴謹態度，並給我許多空間來進行研究，更在適當時機，提醒要有專注的主題，我才能有初步的結果，老師，非常謝謝你。感謝張晃猷老師，上張老師的課，讓我對生物科技有較深的認識，更感謝張老是在論文和工作上的建議。感謝邱顯泰老師，上老師的生化課，老師的認真、專業的態度讓我收穫很多，也感謝邱老師抽空擔任我的口試主持人，更給了我許多寶貴的建議。在實驗上，感謝靖婷學姊，在開始時，帶了我許多的實驗，讓我可以順利進入實驗的正軌；感謝盈璁學長，在許多實驗問題、想法上，給了許多幫助和建議；感謝怡琪學姊，提供了我莢膜的多株抗體，讓我在實驗上有了進展；感謝丸子學姊，除了在實驗上的建議，更感謝你分擔我情緒上的壓力；感謝小新的協助，除了實驗室的工作上幫我很多，更在實驗方面給了我許多的意見和激盪。感謝榕華學姊、同學珮瑄、婉君，學弟佑俊、健誠、育聖、士毅、學妹欣穎在實驗和生活上的幫忙，謝謝智凱幫我處理畢業的事。感謝女友佩娟幫我分擔生活、實驗的壓力，讓我可以順利完成兩年的碩士學業。

Contents---------- 2

Abstract---------- 3

Introduction---------- 5

Materials and Methods---------- 12

Results---------- 18

Discussion---------- 23

References---------- 26

Table---------- 32

Figure---------- 38

Appendix---------- 55

中文摘要

蛋白質酪胺酸的磷酸化，在真核生物的生理作用中扮演重要的調控角色，長久以來被認知。然而，在原核生物中的功能和重要性卻仍待釐清。本實驗室的研究對象-克雷白氏肺炎桿菌，具有厚實的莢膜，為此菌引起感染的重要因子。先前研究已發現，負責合成莢膜的基因組中含有一個酪胺酸激酶-Yco6 和一個去磷酸酶-Yor5。本研究的目標在釐清 Yco6 和 Yor5 的交互作用，並分析此作用如何影響克雷白氏菌 CG43 K2 血清型的莢膜生成。首先，我們分別建構了 *yor5* 和 *yco6* 的缺損突變株；進一步利用西方轉印法分析，我們證明兩個突變株的莢膜多醣體（CPS）皆明顯減少；此外，結合西方轉印法和阿爾新藍-銀染法的分析結果，我們發現這兩個基因的缺陷也會影響莢膜多醣體形成時的聚合作用。同時，我們利用大腸桿菌系統來表現和純化 Yor5、Yco6 和莢膜多醣體基因組中的重組蛋白質，由硝基苯酚磷酸鹽（pNPP）的分解作用，我們證實重組蛋白質 Yor5 的去磷酸酶活性；而利用體外的去磷酸化實驗，我們也證明 Yor5 會調控 Yco6 的磷酸化程度；在尋找 Yco6 目標蛋白質的磷酸化實驗中，我們初步發現位在莢膜多醣體基因組的 Orf1, Orf3,和 Orf15 及 Ugd 不被 Yco6 所磷酸化。更進一步，我們利用免疫沉澱法，在全菌體蛋白質中發現可受 Yco6 磷酸化的蛋白質，而這些蛋白質仍待分析確認。

Abstract

The phosphorylation of proteins at tyrosine residues has long been known to play a key role in the control of numerous fundamental functions in eukaryotes. In contrast, the biological significance of the protein-tyrosine phosphorylation is not clear in prokaryotes. It has been demonstrated that Yco6 is a tyrosine kinase and Yor5 is a phophatase in the capsule synthesis operon of *Klebsiella pneumoniae*, an opportunistic pathogen with a heavy capsule as an important virulence factor. In this study, we intend to demonstrate how the Yor5/Yco6 pair affects the capsule production in *Klebsiella pneumoniae* CG43 of K2 serotype. Firstly, we have constructed respectively *yor5* and *yco6* deletion mutants. The two mutants appeared to reduce significantly the production of capsular polysaccharides (CPS) as demonstrated by Western blot analysis with an anti-K2 antibody. Using alcian blue-silver stain to analyze the CPS, we have shown that the mutants most likely affect polymerization of the CPS. Secondly, Yor5, Yco6 and some of the genes encoding CPS operon were over-expressed respectively in *E. coli* and the recombinant proteins purified by a nickel-resin affinity column. The phosphatase activity of Yor5 was demonstrated by its capability to decompose *p*-nitrophenyl phosphate (PNPP). Using an *in vitro* dephosphorylation assay, we have shown also that Yor5 can regulate the phosphorlation level of Yco6. Subsequently, *in vitro* phosphorlation assay showed that Orf1, Orf3 and Orf15 in K2 *cps* gene cluster and Ugd are not the targets of Yco6. Finally, immunoprecipitation employed to search for the targets of Yco6 has identified several likely target proteins and the identities remain to be verified.

Introduction

Klebsiella pneumoniae, a member of the *Enterobacteriaceae*, is a rod-shaped and highly encapsulated bacterium which is often present as a saprophyte in nasopharynx and in intestinal tract. It is also an important cause of community-acquired disease including pneumonia, bacteremia, septicemia, urinary tract and respiratory infections, occurring particularly in immunocompromised patients (Podschun *et al*., 1998). The current research of *K. pneumoniae* revealed a series of virulence factors including capsular polysaccharide, which protects the bacterium from phagocytosis and also preventing from killing by serum factors (Simoons *et al*., 1986)；lipopolysaccharides, consisted of lipid A, core and O antigens, are essential for bacteria to resist complement-mediated killing (Alberti *et al*., 1996)；siderophores that are capable of iron chelating (Chart *et al*., 1988)；pili (fimbriae) which bind specifically to the receptors on cellular surface prior infection (Fader *et al*., 1979).

Thick capsule is a representing feature of *K. pneumoniae* and at least 77 distinct serotypes have been classified in the bacteria (Mizuta *et al.*, 1984). On the basis of mouse lethality assay, the strains belonging to serotypes K1 and K2 were found to be the most virulent (Simoons *et al*., 1986). *K. pneumoniae* CG43, a clinical isolate of K2 serotype, showing a strong virulence to Balb/c mice with 50 % lethal dose as low as 10 CFU has been demonstrated in our laboratory (Chang *et al*., 1996). In *Escherichia coli*, CPS can be classified into four groups by their chemical and physical criteria. The group I of a high molecular mass contains uronic acid as the acidic component and is coexpressed with specific O polysaccharides (Whitfield *et al.*, 1999). The structure of *K. pneumoniae* K2 CPS has been determined as [→)

4-Glc-(1→3)-α-Glc-(1→4)-β-Man-(3←1)-α-GlcA)-(1→] $_n$ (Wacharotayankun et al., 1992), which is made from a similar biosynthetic pathway to that of the *E. coli* group I CPS (Whitfield *et al*., 1999).

The gene cluster *cps* (*c*apsular *p*olysaccharide *s*ynthesis) region that is responsible for K2 CPS synthesis of *K. pneumoniae* Chedid has been determined, which contains a total of 19 open reading frames organized into 3 transcriptional units as shown in Appendix 1 (Arakawa *et al*., 1995). As shown in Appendix 2, *orf1* is a UTP-glucose-1-phosphate uridylyltransferase homolog; *orf2* is predicted as a membrane associated phospholipid phosphatase; *orf3* is homologous to the gene product required for surface expression of *E. coli* group 1 K antigen; *orf4* is a Wza homolog, which is a periplasmic protein involved in polysaccharide export; *orf5*, Yor5, is a low molecular weight phosphatase; *orf6*, Yco6, is a protein tyrosine kinase; *orf7* and *orf8* are glycosyltransferase homologs; *orf9* is a likely mannosyltransferase; *orf10* is a CapD homolog required for the biosynthesis of type 1 capsular polysaccharide (Hoskins *et al*., 2001); *orf11* is a Wzx homolog, which is likely a flippase involved in the export of O-antigen and teichoic acid (Pausen *et al*., 1997); *orf12* is a hypothetical protein of 65.4 kDa; *orf13* is an acetyltransferase homolog; *orf14*, is a glycosyltransferase homolog; *orf15* is a homolog of gluconate-6-phosphate dehydrogenase; *orf16* is a mannose-1- phosphate guanylyl-transferase homolog; *orf17* is a phosphomannonutase dehydro- genase homolog ; *orf18* and *orf19* are homologous to transport proteins.

In recent years, significant advances have been made in our understanding of the mechanisms involved in regulation, assembly and transport of capsular polysaccharide. The assembly and transport mechanisms of bacterial capsular

polysaccharide have been divided into two types: Wzy-dependent system and ATP binding cassette (ABC) transporter-dependent system (Whitfield *et al*., 1999). The former, originally described for biosynthesis of *Salmonella* serogroups B, D and E O antigens, is responsible for polymerization and transmembrane export of the group 1 and 4 capsules. Individual repeat units are assembled on a carrier lipid (undecaprenyl phosphate) by the sequential activities of serial glycosyltransferase enzymes (Clarke, 1995). The lipid-linked repeat units are then transferred across the plasma membrane by Wzx protein, using a mechanism that had yet to be established (Paulsen *et al*., 2003; Yoshida *et al*., 2003). Sequence similarity placed Wzx into a family of polysaccharide exporter proteins recently designated polysaccharide specific translocation-PST (Paulsen *et al*., 1997). Polymerization of the lipid-linked repeat units at the reducing terminus, one repeat unit at a time, appears to occur at the periplasmic face of the plasma membrane and is catalyzed by the polymerase enzyme, Wzy (Drummelsmith and Whitfield, 1999). In contrast, polymerization and export of the group 2 and 3 capsules by ABC transporter-dependent systems take place on the cytoplasmic face of the plasma membrane, which also involve a sequential action of glycosyltransferases to elongate the polysaccharide at the non-reducing end. The nascent polysaccharide is then transported across the plasma membrane by an ABC-2 transporter. In the case of group 2 capsules, this transporter comprises KpsM, the transmembrane component and KpsT, the ATPase component (Pavelka *et al.*, 1994; Russo *et al*., 1998).

The regulatory strategy of colanic acid biosynthesis employed by *E. coli* usually serves as a model for group I CPS synthesis (Stout *et al*., 1991). It is built by the RcsC/YojN/RcsB two-component regulatory pair, which involved a multistep signaling transduction. The RcsC hybrid sensor kinase senses certain environmental

stimuli and the signal relayed to the downstream signaling component YojN (a histidine-containing phosphotransfer HPt factor), which serves as an intermediate for the phosphorelay. Eventually, the RcsB response regulator acquires the phosphoryl group from YojN. The phosphorylated RcsB functions as a DNA-binding transcriptional regulator, which together with RcsA activate the transcription of the *cps* genes for CPS production. In addition to RcsB regulator, the *rmpA2* locus in pLVPK (for Large Virulence Plasmid in *Klebsiella*) was also demonstrated as an alternative activator for CPS biosynthesis in *K. pneumoniae* CG43 (Lai *et al*., 2003). In additional, the *cps* gene cluster of CPS group 1 contains a highly conserved block of three genes, *wza-wzb-wzc*, which were originally identified in *E. coli* K30 (Drummelsmith *et al*., 1999). The three genes encode respectively an outer membrane lipoprotein (Wza), a cytoplasmic tyrosine phosphatase (Wzb) and a tyrosine kinase (Wzc). The orthologous genes have also been described in a diverse system including *E. coli* K-12 (Stevenson *et al*., 1996), *Erwinia amylovora amsH, amsI* and *amsA* (Bugert and Geider, 1995), *K. pneumoniae orf4-yor5-yco6*. The conserved tyrosine kinase in *cps* gene cluster suggests a regulatory role of tyrosine phosphorylation in bacterial CPS formation.

In eukaryotes, a plethora of protein-tyrosine kinases and phosphotyrosine-protein phosphatases that catalyze the reversible phosphorylation on tyrosine residues of proteins have been detected; they have been shown to be critical in the regulation of various important biological functions, including signal transduction, growth control, and malignant transformation (Fantl *et al*., 1993). In contrast, only a few reports described the functional roles of tyrosine protein phosphorylation in prokaryotes. Phosphorylation on tyrosine of bacterial proteins has been reported for the first time by purifying a particular phosphoprotein, Ptk from *Acinetobacter. johnsonii* (Cortay *et*

al., 1986). An autokinase activity of PTK was later demonstrated in vitro at the expense of ATP (Vincent *et al*., 1999). The mechanism of autophosphorylation of Wzc, a tyrosine kinase in *E. coli* K-12, was also demonstrated (Grangeasse *et al*., 2002). The tyrosine kinase, which is a protein of 720 amino acids bound to the inner membrane of bacteria, consists of two functional domains: a C-terminal domain that contains the tyrosine kinase activity and an N-terminal transmembrane domain. Tyrosine phosphorylation occurs at the expense of ATP molecules that bind to Walker A and B motifs of the C-terminal domain. This domain contains six phosphorylation sites; five of these sites are located at the extreme C-terminus of the molecule in the form of a tyrosine cluster, and one is located further upstream, at Y569. It has been shown that Y569 can firstly autophosphorylate through an intramolecular reaction that induces an enhanced kinase activity of Wzc, which in turn, results in the phosphorylation of the five terminal tyrosine residues by an intermolecular process (Grangeasse *et al.*, 2002). Phosphotyosine protein phosphatase, Wzb, is able to specifically dephosphorylate the cognate protein- tyrosine kinases, thus plays a possible regulatory role for tyrosine phosphorylation.

Some reports provide evidence to show that the activity of those protein tyrosine kinases is associated with virulence and production of the exopolysaccharide (Ilan *et al*., 1999). The phosphorylation of *E. coli* tyrosine autokinase Wzc appeared to be essential for the assembly of group I capsular polysaccharides (Wugeditsch *et al*., 2001). When this protein is phosphorylated, the production of the particular exopolysaccharide, colanic acid, is blocked. The production of colanic acid starts again when Wzc is dephosphorylated by its cognate phosphoprotein phosphatase, Wzb (Vincent *et al*., 2000). The tyrosine-cluster of Wzc also plays an important role in capsular polysaccharide production. The *wzc* mutant lacking the tyrosine cluster is

defective in producing capsular polysaccharide. Deletion of any two tyrosine residues of the tyrosine-cluster appeared to show the effect on capsular polysaccharide production. However, deleting each one of the tyrosine residues in the cluster revealed no obvious effect in the synthesis of capsular polysaccharide (Paiment *et al*., 2002). It is believed that the phosphorylation degree of the tyrosine cluster affect the production of capsular polysaccharide.

It has been demonstrated that Wzc can oligomerize to form essentially trimers and hexamers by *in vivo* cross-linking experiments. It was suggested that the oligomerized Wzc plays a role in capsular polysaccharide translocation **(**Doublet *et al*., 2002**).** Wza can also form a multimeric complex in the outer membrane for translocation of the group 1 capsular polysaccharide to *E. coli* surface. It have been demonstrated that Wza is able to form a protein complex with Wzc to help for the CPS translocation (Nesper *et al*., 2003). Not until very recently, UDP-glucose dehydeogenase was identified as a target of Wzc kinase using *in vitro* phosphorylation assay (Grangeasse *et al*., 2003). It was showed that Ugd could be phosphorylated by Wzc and the phosphorylation enhances its enzyme activity to affect LPS and colanic acid production.

A hypothetic model (Rahn *et al*., 2003) has recently been proposed to explain the fuctional roles of Wza, Wzb, Wzc, Wzx and Wzy. Step A-glycosyltransferases synthesize undecaprenol pyrophosphate (und-PP)-linked repeat units at the cyto-plasmic face of the inner membrane. Step B-the und-PP-linked repeat units are flipped across the inner membrane by a process involving Wzx. Step C-the repeat units are polymerized in a Wzy-dependent reaction. Step D-Wzc undergoes autopho-sphorylation, followed by transphosphorylation between proteins in an oligomeric

form, to enhance further polymerization. Step E-dephosphorylation of Wzc by the Wzb phosphatase is also crucial for capsule synthesis. Step F-exportation of the polymer to the surface requires the outer memebrane Wza multimeric complex, as an export channel. Step G-Wzi is required for an efficient assembly of the capsular layer.

Accordingly, we propose in Fig. 1 that: **(**1) Yor5 regulates the Yco6 phosphorylation level without alternation of the kinase activity; (2) Yco6 phosphorylates the CPS synthesis enzymes and hence affects CPS production; (3) Yor5 affects CPS polymerization by regulates the interaction of Yco6 and Wzx. In the study, we aim to validate the hypothesis, and the proposed experiments are as following:

1. Construction of *K. pneumoniae* CG43 *yor5, yco6* and *wzx* mutants and the capsular polysaccharide production of the mutants are compared.
2. Using *in vitro* dephosphorylation assay to confirm the interaction between Yor5 and Yco6.
3. Identification of the target proteins phosphorylated by Yco6 with anti-phospho-tyrosine monoclonal antibody.
4. Using *in vitro* phosphorylation assay to demonstrate if Ugd or any one of the *cps* gene products is the target of Yco6.

Materials and methods

Plasmids, bacterial strains, and growth conditions. The bacterial strains and plasmids used in this study are listed in Table 1 and Table 2 and *K. pneumoniae* CG43 is a clinical isolate recovered from a patient in the Chang Gung Memorial Hospital, Linkou. The bacteria were propagated at 37 ° C in Luria-Bertani (LB) broth or the medium supplemented with appropriate antibiotics which include kanamycin (25 μg/ml), ampicillin (100 μg/ml) and tetracycline (20 μg/ml).

Nucleotide sequence analysis. Homology search analysis and alignment were performed with BlastP analysis in NCBI (http://www.ncbi.nlm.nih.gov). Signal sequences in the predicted amino acid sequenceswere found by SignalP 3.0 (Jannick *et al*.,2004) and LipoP 1.0 (Juncker *et al*.,2003). Transmembrane regions in the predicted amino acid sequences were predicted by TopPred 2 (Gunnar von Heijn, 1992).

Construction of *yor5, yco6, wza* and *wzx* deletion mutants. *K. pneumoniae* CG43 mutants disrupted specifically at *yor5*, *yco6*, *wza*, or *wzx* genes were constructed by the allelic exchange strategy. The primer sets used for PCR amplification of the DNA fragments flanking sequence are listed in Table 3. The generated DNA fragments were cloned into pKAS46, a suicide vector (a generous gift of K. Skorupski, University of New Hampshire), and the resulting plasmids were then mobilized to *K. pneumoniae* CG43S3 through conjugation from *E. coli* S17-1 λ *pir*. The trans-conjugants were selected with kanamycin on minimal medium. Some of the kanamycin-resistant transconjugants was picked and then spread onto a LB plate supplemented with streptomycin (500 μg/ml). After the occurrence of a double cross-

over, the streptomycin-resistant and kanamycin-sensitive colonies were isolated, and the deletions of *yor5*, *yco6*, or *wzx* were verified by PCR and by Southern blot analysis with a gene specific probe.

Quantification the glucuronic acid content. The CPS was extracted by using the method described previously (Domenico *et al*., 1989). Briefly, bacteria were collected from 500 μl of culture and mixed with 100 μl of 1% Zwittergent 3-14 detergent (Sigma-Aldrich, Milwaukee, WI) in 100 mM citric acid (pH2.0). The mixture was incubated at 50°C for 20 min. After centrifugation, 250 μl of the supernatant was transferred to a new tube and CPS was precipitated with 1 ml of absolute ethanol. The pellet was then dissolved in 200 μl distilled water and a 1,200 μl of 12.5 mM borax (Sigma-Aldrich, Milwaukee, WI) in H_2SO_4 was added. The mixture was vigorously vortexed, boiled for 5 min, cooled, and then 20 μl of 0.15% 3-hydroxydiphenol (Sigma-Aldrich, Milwaukee, WI) was added and the absorbance at 520 nm was measured. The uronic acid content was determined from a standard curve of glucuronic acid (Sigma-Aldrich, Milwaukee, WI) and expressed as μg per 10^9 CFU.

The purification of capsular polysaccharides. Capsular polysaccharides were purified as described previously (Whitfield *et al*., 1992). Briefly, cells were harvested from LB broth grown for 16 h. The cells were pelleted at 13,200 rpm for 10min and the supernatant was removed. The pellet was resuspended with 500 μl PBS, extracted with hot-phenol and then dialyzed against water over night. The crude extract are treated with DNase (4 mg/ml), RNase (0.2 mg/ml) and proteinase K (4 mg/ml) and dialyzed against water again.

Analysis of capsular polysaccharide. The amount of CPS was determined by dot blot assay. A two fold serial dilution of the CPS extracted from wild and the mutants were immobilized on a polyvinylidene difluoride (PVDF) membrane. The CPS was detected with an anti-K2 polyclonal antiserum and an alkaline phosphatase-conjugated anti-mouse antibody. The intensity was estimated by relative densitometric analysis of the reaction with the ScanAlyze analysis system which was developed by Michael Eisen of Stanford University.

The CPS were then analyzed by electrophoresis on 5% or 10% DOC-PAGE and then transferred to a PVDF membrane for immunoblotting and the polysaccharides detected likewise. The CPS pattern wsa also analyzed with alcian blue-silver stain as described (Reuhs *et al.*, 1998). After electrophoresis, the gel was immediately immersed in 100 ml of alcian blue solution (0.005% alcian blue in 40% ethanol-5% and gently rocked for 30 min. This was followed by a change to 100 ml of fresh solution and overnight rocking. The gel was rinsed for 5 min in dH_2O, oxidized in 100 ml of 0.7% sodium metaperiodate (in dH_2O) for 10 min, and washed five times in 200 ml of dH_2O for 5 min each time. One milliliter of the final wash was added to 1 ml of the 10% silver solution (BIO-RAD 161-0444). The gel was washed two more times if a precipitate formed. Then, the gel was stained in 100 ml of silver solution (10% Bio-Rad silver concentrate) for 10 min and rinsed in dH_2O for 5 min. The gel was rinsed again in 100 ml of Bio-Rad developer (3.0 g/200 ml of dH2O) with agitation until dark precipitate formed and immediately drained to remove all precipitate. Finally, the color was developed with the remaining developer for 5 min. The development was stopped in 100 ml of 5% acetic acid for10 min followed by a 200 ml dH_2O.

Expression and purification of the recombinant Yor5, Yco6E22, Yco6E23, UGD, ORF1 and ORF15. The coding region of *yor5* was PCR amplified with primers Yor3 and Yor4 (Table 3) and the product cloned into *Eco*RV/*Sac*I fragment of pET30b (Novagen, Madison, Wis.). The resulting plasmid pET-Yor5 allows inframe fusion of the *yor5* coding region to six histidine codons at the N terminus and the transcription from a T7 promoter. Cells were grown to mid-exponential growth; expression of Yor5 was induced by addition of 1 mM isopropyl-1-thio-β-D-galactopyranoside (IPTG). The overexpressed His-Yor5 protein was then purified from the soluble fraction of *E. coli* NovaBlue (DE3) carrying pET-Yor5 cell lysate by affinity chromatography with His-Bind resin (Novagen). The purified Yor5 was then concentrated and dialyzed against A buffer (50 mM Tris-HCl, pH 7.4 , 100 mM NaCl, 1 mM EDTA), and the purity was determined by SDS-PAGE analysis. Yco6E22, Yco6E23, Ugd, Orf1 and Orf15 were prepared and purified likewise. Their primers, cloning sites and expression vector were shown at Table. 2. The purified Yco6E22 and Yco6E23 were concentrated and dialyzed against the buffer (10 mM sodium phosphate pH7.4, 150 mM NaCl, 1 mM EDTA, 10% glycerol). Whereas, the purified UGD, ORF1 and ORF15 were concentrated and dialyzed against PBS.

Phosphatase activity assay. The acidic phosphatase activity to detect the formation of *p*-nitrophenol from *p*-nitrophenyl phosphate (PNPP) was monitored at 37°C by using a method as descirbed (Preneta *et al*., 2002) The dephosphorylation rates were determined at 405 nm in a reaction buffer containing 100 mM sodium citrate (pH 6.5), 1 mM EDTA and 10 mM PNPP. The amount of *p*-nitrophenol released was estimated by using a molar extinction coefficient e405 of 18,000 M^{-1} cm^{-1} (Cirri *et al*., 1993).

***In vitro* phosphorylation assay.** In vitro phosphorylation using about 3 mg of the purified His-Yco6E22 and His-Yco6E23 protein were performed at 37°C in 200 µl of a buffer containing 25 mM Tris-HCl (pH 7.0), 1 mM DTT, 5 mM $MgCl_2$, 1 mM EDTA and 5 µCi of [γ-p^{32}] ATP. After 30 min of incubation, the reaction was stopped by addition of an equal volume of 2X sample buffer, and the mixture was heated at 100°C for 5 min. One-dimensional gel electrophoresis was performed using 12.5% SDS polyacrylamide gel and the gels were stained with Coomassie blue while the gels were detected by InstantImager™ (Packard Instrument Company). *In vitro* phosphorylation assay was also used to identify if Orf1, Orf3, Orf15 and Ugd are the targets of Yco6. About 10 mg of Orf1, Orf3, Orf15 and Ugd respectively was incubated with Yco6E23 for 30 min. The reaction was stopped and detected likewise.

Dephosphorylation assay. Dephosphorylation using about 0.1 mg of purified Yco6E22 and Yco6E23 protein was performed as the above described. After 10 min of incubation, dephosphorylation assay of Yco6E23 was carried out with 0.2 mg of purified Yor5 at 37 °C for 2 to 30 min in 30 µl of buffer consisting of 100 mM sodium citrate (pH6.5) and 1 mM EDTA. The reaction was stopped by addition of an equal volume of 2X sample buffer, and the mixture was heated at 100 °C for 5 min. The Yco6E22 and Yco6E23 protein was separated by gel electrophoresis and analyzed by autoradiography. The radioactive bands were excised, and their radioactivities were detected by InstantImager™ (Packard Instrument Company).

I**mmunoblot analysis of the phosphotyrosine proteins.** The whole cell protein lysates was analyzed using 12.5% SDS PAGE gels and the resolved proteins were transferred to a polyvinylidene difluoride (PVDF) membrane electrophoretically. The

transfer buffer contains 137 mM NaCl, 2.7 mM KCl, 10 mM Na_2HPO_4, 2 mM KH_2PO_4 and 20% methanol. The phosphotyrosine proteins were detected using anti-phosphotyrosine monoclonal antibody with an anti-mouse AP conjugate (Sigma P3300) as the secondary antibody. The bound antibody was detected by using nitro blue tetrazolium chloride/5- bromo-4-chloro-3- indolyl phosphate.

Immunoprecipitation. Cells were harvested from 3 ml LB broth grown for 16 h. The cells were pelleted at 13,200 rpm for 10min and the supernatant was removed. The pellet was resuspended with 500 µl IP buffer containing 50 mM Tris-HCl (pH7.5), 150 mM NaCl and 1% Triton-X100 to sonicate. The total proteins of the samples collected from the soluble fraction were regulated to equal, and then add 15 µl protein A/G (Santa Cruz Biotechnology sc2003) to precleaning at 4 °C for 4 h. The mixes were centrifuged at 10,000 rpm for 5 min. Add 4 µl anti-phosphotyrosine antibody-conjugated agarose (Sigma PT66) to be mixed at 4 °C overnight. Then 50 µl protein A-G was added to be mixed for 4 h to catch the target proteins-antibody conjugants. The proteins were pelleted at 10,000 rpm for 5 min and then 40 µl sample buffer was added to heat 100 °C for 10min. The proteins were resolved by 12.5% SDS-PAGE.

Preparation of anti-Yor5, Yco6 and Wza polyclonal antibody. BALB/c mice were immunized using Yor5, Yco6 and Wza. Aliquots of this material containing 100 µg of these proteins were emulsified 1:1 in Freund's complete adjuvant. After ten days, the material of equal proteins emulsified 1:1 in Freund's incomplete adjuvant was injected into the mouse again. Serum samples showed a strong anti-Yor5, Yco6E23 and Wza, as assessed by ELISA.

Result

Comparative analysis of the *K. pneumoniae cps* gene clusters. The K2 *cps* gene cluster of *K. pneumoniae* Chedid has been sequence determined, which is consisted of 19 open reading frames organized into 3 transcriptional units has been identified (Appendix 1). *K. pneumoniae* CG43, as well as *K. pneumoniae* Chedid, produce capsular polysaccharide of K2 serotype (Chang *et al*., 1996). Comparative analysis of the *cps* gene cluster of Chedid, NTUH-K2044 with K1 serotype, and WCG78578 with unknown serotype used BLASTP program revealed eight core components shown in Fig. 2 and Table 4. The *orf18* and *orf19* in Chedid *cps* gene cluster appeared to be the orf18 in that of NTUH-K2044. We also have found the eight conserved genes which encode respectively UTP-glucose-1-phosphate uridylyltransferase, ORF2, ORFX, Wza, Yor5, Yco6, Wzx and 6-phosphogluconate dehydrogenase while using a Blastp search , homology search allowed us assign the functions of the *cps* genes (Table 4). The features of the eighteen ORF were described as shown in Table 5.

Construction of *yor5* and *yco6* mutants. To demonstrate that the functional roles of Yor5 and Yco6, we have constructed the *yor5* and *yco6* deletion mutants. As shown in Fig. 3A, 650-bp signal was obtained in the mutant while using Yor5 gene as the probe, indicated an expected deletion of *yor5*. PCR using the primer pair Yco6E1 and Yco6E4 amplified a 2200-bp product in wild type strain and a 400-bp fragment in CG43-S3-yco6^{-}. The *yco6* deletion in the mutant strain was further demonstrated by Southern blot analysis using the probe encoding the Yco6 (Fig. 3B).

Characterization of the *yor5* and *Yco6* deletion mutants. To investigate the role of Yor5 and Yco6 in K2 CPS biosynthesis, the *K. pneumoniae yor5 and yco6* deletion mutants were generated. We have found that the mutant strains displayed a smaller

colony morphology on LB agar compared to the wild type strain. The mucoidy of the mutants appeared to be significantly reduced as determined by string formation. The loss of mucoidy was also evident when the bacterial cultures were subjected to low-speed centrifugation. As shown in Fig. 4A, both CG43S3-*yor5*$^-$ and CG43S3-*yco6*$^-$ cells were precipitated much faster than the strain CG43S3. Besides the mucoidy phenotypes, both mutants showed a higher growth rate than wild type in LB broth (Fig. 4B).

Yor5 and Yco6 are involved in the regulation of K2 capsule. To compare the CPS production in CG43S3, CG43S3-*yor5*$^-$, CG43S3-*yco6*$^-$ and U9451, dot blot probed with anti-K2 polycolonal antibody showed that the CPS amount of CG43S3 is about four-time neither eight-time than that of CG43S3-*yor5*$^-$ and CG43S3-*yco6*$^-$, respectively (Fig. 5). The result indicated that both *yor5* and *yco6* affect the bacterial CPS production. To further analyze the mutation effects, the amount of CPS in CG43S3, CG43S3-*yor5*$^-$ and CG43S3-*yco6*$^-$ were determinated by measuring the content of glucuronic acid, which serves as an indicator of K2 CPS (Vodonik SA and Gray GR, 1988). As shown in Fig. 6, the glucuronic acid amounts of that CG43S3-*yor5*$^-$ and CG43S3-*yco6*$^-$ appeared to reduce approximately three fold comparing to CG43S3. The mutations of *yor5* and *yco6*, as demonstrated in Fig. 7, also affect CPS pattern. In either CG43S3-*yor5*$^-$ or CG43S3-*yco6*$^-$, the high molecular weight fraction of CPS disappeared in CG43S3 as demonstrated by immune blot analysis using anti-K2 antiserum (Fig. 7A) The changes from polymeric form to oligomeric form in CG43S3-*yor5*$^-$ and CG43S3-*yco6*$^-$ were also confirmed using alcian blue-silver staining of the CPS (Fig. 7B). In order to further analyze the mutant effects of these mutations on oligomeric CPS, the CPS samples were applied to 10%

DOC PAGE. As shown in Fig. 8, wild-type and two mutants revealed a similar CPS ladder pattern indicating that the mutation at either *yor5* or *yco6* does affect the synthesis of CPS oligomer in *K. pneumoniae*.

In vitro autophosphorylation of Yco6 and its dephosphorylation by Yor5

To demonstrate the interaction between Yor5 and Yco6, we have overexpressed both genes in *E. coli* and purified the recombinant Yor5 and Yco6E23. Yco6E23 contains only kinase domain of Yco6, is soluble for purification. As showed in Fig. 9, the protein resolved by SDS-PAGE is of more than 90% purity as determinated by Coomassie Blue staining. To assess phosphatase activity of the recombinant His_6-Yor5, we carried out a *p*-nitrophenyl phosphate (pNPP) decomposition assay, which was monitored at 37°C by detecting the formation of *p*-nitrophenol from PNPP (Fig. 10A). The dephosphorylation rate of His_6-Yor5 calculated is 3.2×10^{-7} moles/min/mg determined at 405 nm (Fig. 10B). On the basis of Coomassie Blue-staining, the recombinant Yco6E23 appeared to be not soluble (Fig. 11A). We then combine with sorbitol-betaine induction at low temperate and the concentration of imidazole in the wash step to increase solubility of recombinant His_6-Yco6E23. As shown in Fig. 11B, the protein purity reached more than 80%. The purified Yco6E23 showed an autokinase activity by incorporating the [γ-p^{32}] ATP after 30 min incubation and then the phosphorylated Yco6E23 appeared to be dephosphorylated by Yor5 in a time-dependent manner (Fig. 12).

Yco6E23 is able to form a dimerized complex.

As shown in Fig. 12, a high-molecular band was found which likely represents the hetero-complex between Yor5 and Yco6E23 or an Yco6E23 homodimer. The strength of complex formation appeared to be high, which is able to resist SDS treatment. We

then performed a Western blot with anti-phosphotyrosine monoclonal antibody and anti-His tag monoclonal antibody to investigate the possibility. We have proved that Yco6E23 is able to form a SDS-resistant dimmer which also showed a certain degree of heat-resistant (Fig. 13).

Identification of the Yco6 Target proteins in *K. pneumoniae* CG43

The above mentioned experiments suggest that Yco6 is able to regulate CPS synthesis enzymes through phosphorylation. Western bolt of whole cell lysate probed with anti-phosphotyrosine monoclonal antibody (Sigma P3300) was therefore used for the target protein identification. The phosphorylated Yco6, which of the predicted molecule weight is approximately 80 kDa disappeared in CG43S3-*yco6*$^-$ as shown in Fig. 14. In addition, five phosphorylated proteins were found to be missing in CG43S3-*yco6*$^-$. In order to resolve better for isolation of the target proteins, immunopreciptation was used with anti-phosphotyrosine monoclonal antibody (Sigma PT 66), which is suitable for immunopreciptation. The resolution again appeared to be poor; however, several missing bands were still been identified.

Identification of the likely targets of Yco6 in the *cps* gene cluster.

We intended to overexpress the entire *cps* gene cluster in *E. coli* and purified the recombinant proteins of the following. However, we have only successfully overexpress Orf1, Orf3 and Orf15 in *E coli* as shown in Fig. 16, in addition to Ugd, which have been reported recently that Wzc can phosphorylate Ugd to increase its enzyme activity (Grangeasse, 2003). His_6-ORF1 appeared to be insoluble protein, the soluble proteins; His_6-ORF1, His_6-ORF15 and His_6-Ugd were subsequently purified for phosphorylation assays as seen in Fig. 17. The phosphorylation assay revealed that

none of Ugd, Orf3 and Orf15 is the target of Yco6.

Disscusion

Comparative analysis of the *cps* gene clusters of *K. pneumoniae* Chedid, MCG 78578 and NTUH-K2044 revealed at eight conserved genes including *orf1*, *orf2*, *orfX*, *wza*, *yor5*, *yco6, wzx* and *orf15* (Table 4 and 5). Four of them, OrfX, Wza, Yor5 and Yco6 have also been identified in many serotypes of *E. coli* (Rahn *et al*. 1999). The conserved *orfX-yco6* region represents the feature of group 1 capsule clusters and distinguishes all of them from the gene clusters of group 4 capsules and O antigens (Whitfield and Roberts, 1999). Another important feature of group 1 capsule is the Wzy-depnedent system, which includes the basic components, Wzx (flippase) and Wzy (polymerase). It is likely that Wzy is a highly diversed protein because we were unable to assign a Wzy homolog in either of three *K. pneumoniae* strains by using a sequence similarity search. The conserved *orf1* encoding UTP-glucose-1-phosphate uridylyl- transferase, *orf2* and *orf15* encoding 6-phosphogluconate dehydrogenaseare are likely playing similar role in affecting the CPS synthesis in the three strains. The genes located downstream of Yco6 are highly variable, which encode respectively glycosyl- transferase and sugar nucleotide synthetic enzymes. The variable genes are most possible the key determinants of the capsule serotype.

In this study, the functional roles of Yor5 and Yco6 in capsule formation of capsular polysaccharide synthesis in *K. pneumoniae* CG43 were investigated. We have demonstrated that the phosphatase-Yor5 and autokinase-Yco6 are both involved in *K. pneumoniae* CG43. Yor5 and Yco6 encoding genes located within the *cps* gene cluster in *K. pneumoniae* appeared to affect both synthesis and polymerization of the CPS. The *yor5* and *yco6* deletion mutants both showed less colony mucoidy and a higher growth rate, which is likely due to switching off the nutrient-demanding process for

CPS synthesis. Further analysis of the CPS content showed that the production of CPS in wild type is much higher than that of the mutants. We have demonstrated that Yor5 is capable of dephosphorylating Yco6, which supports the model that Yor5 plays a regulatory role in the phosphorylation level of Yco6. The dephosphorylated Yco6 can again be phosphorylated by its autokinase activity. The conserved features in Yco6 homologues suggest a shared and widespread role in prokaryotes (Appendix 2). Since many of the kinase-containing bacteria require capsular or extracellular polysaccharides as essential virulence determinants, Yco6 homologues play a crucial role in pathogenesis of these organisms. Regulation by a post-translational phosphorylation event represents a new dimension in the assembly of bacterial cpaular polysaccharides. Thus, the interaction between Yor5 and Yco6 might be cyclic in order to control translocation or assembly of CPS.

Interestingly, the two mutants not only showed a significant reduction of CPS, but also decreased the formation of high molecule weight CPS. In *E. coli* group 1 K30 serotype, Wzb and Wzc have also been demonstrated to affect CPS assembly (Drummelsmith and Whitfield, 1999). However, the mechanism remains to be investigated. Many studies of O-antigen revealed that many bacterial strains can efficiently translocate both full-length and truncated LPS molecules, which leads to heterogeneity of LPS (Amor and Whitfield, 1997). Translocation of CPS is likely using a different mechanism. We also predicted amino acid sequences by SignalP 3.0 and LipoP 1.0. Transmembrane regions in the predicted amino acid sequences were predicted by TopPred 2. Based on our analysis, most of enzymes involved in CPS synthesis were predicted to locate in cytosol, therefore, we suggest that the CPS repeat units were produced before being translocated to periplasmic space. It is proposed that Yco6 forms a multimer protein to affect CPS translocation, and then

block the polymerization possibly by interacting with Wzx. Yor5 controls the phosphorylation level of Yco6, possibly altering its ability to interact with Wzx, which needs further investigation. Proper alterations between activation and inactivation of Yco6 by Yor5 may thus form a cycle for regulation of CPS translocation.

The protein-tyrosine kinase Wzc of *E. coli* was recently demonstrated to phosphorylate an endogenous enzyme, UDP-glucose dehydrogenase (Ugd), which participates in the synthesis of the exopolysaccharide colanic acid (Grangeasse *et al*., 2003). The phosphorylation of Ugd was demonstrated to actually occur on tyrosine residue, resulting in a significant increase of its dehydrogenase activity. In our study, several possible targets of Yco6 were examined by Western blotting and immunoprecipitation. However, these possible targets of Yco6 that disappeared in *yco6* mutant may be the result of degradation of auto-phosphorylated Yco6. To identify these proteins, we will try to increase the concentration of the target proteins or using silver stain method to improve resolution. The candidates will then be isolated and sequence identified. We will also overexpress other genes of *cps* gene cluster to identify other Yco6 target proteins.

Refernece

Alberti S, Alvarez D, Merino S, Casado MT, Vivanco F, Tomas JM, Benedi VJ. 1996. Analysis of complement C3 deposition and degradation on *Klebsiella pneumoniae*. Infect Immun. 64(11):4726-32.

Amor PA, Whitfield C. 1997. Molecular and functional analysis of genes required for expression of group IB K antigens in *Escherichia coli*: characterization of the his-region containing gene clusters for multiple cell-surface polysaccharides. Mol Microbiol. 26(1):145-61.

Arakawa Y, Wacharotayankun R, Nagatsuka T, Ito H, Kato N, Ohta M. 1995. Genomic organization of the *Klebsiella pneumoniae cps* region responsible for serotype K2 capsular polysaccharide synthesis in the virulent strain Chedid. J Bacteriol. 177(7):1788-96.

Bugert P and Geider K. 1995. Molecular analysis of the ams operon required for exopolysaccharide synthesis of *Erwinia amylovora*. Mol Microbiol. 15(5):917-33.

Chang HY, Lee JH, Deng WL, Fu TF, Peng HL. 1996. Virulence and outer membrane properties of a *galU* mutant of *Klebsiella pneumoniae* CG43. Microb Pathog. 20(5):255-61.

Chart H, Stevenson P, Griffiths E. 1988. Iron-regulated outer-membrane proteins of *Escherichia coli* strains associated with enteric or extraintestinal diseases of man and animals. J Gen Microbiol. 134 Pt 6:1549-59.

Clarke BR, Bronner D, Keenleyside WJ, Severn WB, Richards JC, Whitfield C. 1995. Role of Rfe and RfbF in the initiation of biosynthesis of D-galactan I, the lipopolysaccharide O antigen from *Klebsiella pneumoniae* serotype O1. J Bacteriol. 177(19):5411-8.

Cortay JC, Duclos B, Cozzone AJ. 1986. Phosphorylation of an *Escherichia coli* protein at tyrosine. J Mol Biol. 187(2):305-8.

Cirri P, Chiarugi P, Camici G, Manao G, Raugei G, Cappugi G, Ramponi G. 1993 The role of Cys12, Cys17 and Arg18 in the catalytic mechanism of low-M(r) cytosolic phosphotyrosine protein phosphatase. Eur J Biochem. 214(3):647-57.

Domenico P, Schwartz S, Cunha BA. 1989. Reduction of capsular polysaccharide production in *Klebsiella pneumoniae* by sodium salicylate. Infect Immun. 57(12): 3778-82.

Doublet P, Grangeasse C, Obadia B, Vaganay E, Cozzone AJ. 2002. Structural organization of the protein-tyrosine autokinase Wzc within *Escherichia coli* cells. J Biol Chem. 277(40):37339-48.

Drummelsmith J, Whitfield C. 1999. Gene products required for surface expression of the capsular form of the group 1 K antigen in *Escherichia coli* (O9a:K30). Mol Microbiol. 31(5):1321-32.

Fader RC, Avots-Avotins AE, Davis CP. 1979. Evidence for pili-mediated adherence of *Klebsiella pneumoniae* to rat bladder epithelial cells in vitro. Infect Immun. 25(2):729-37.

Fantl WJ, Johnson DE, Williams LT. 1993. Signalling by receptor tyrosine kinases. Annu Rev Biochem. 62:453-81.

Gottesman, S., and V. Stout. 1991. Regulation of capsular polysaccharide synthesis in *Escherichia coli* K-12. Mol. Microbiol. 5:1599-1606

Grangeasse C, Doublet P, Cozzone AJ. 2002. Tyrosine phosphorylation of protein kinase Wzc from *Escherichia coli* K12 occurs through a two-step process. J Biol Chem. 277(9):7127-35.

Grangeasse C, Obadia B, Mijakovic I, Deutscher J, Cozzone AJ, Doublet P. 2003.

Autophosphorylation of the *Escherichia coli* protein kinase Wzc regulates tyrosine phosphorylation of Ugd, a UDP-glucose dehydrogenase. J Biol Chem. 278(41):39323 -9.

Hoskins J, Alborn WE Jr, Arnold J, Blaszczak LC, Burgett S, DeHoff BS, Estrem ST, Fritz L, Fu DJ, Fuller W, Geringer C, Gilmour R, Glass JS, Khoja H, Kraft AR, Lagace RE, LeBlanc DJ, Lee LN, Lefkowitz EJ, Lu J, Matsushima P, McAhren SM, McHenney M, McLeaster K, Mundy CW, Nicas TI, Norris FH, O'Gara M, Peery RB, Robertson GT, Rockey P, Sun PM, Winkler ME, Yang Y, Young-Bellido M, Zhao G, Zook CA, Baltz RH, Jaskunas SR, Rosteck PR Jr, Skatrud PL, Glass JI. 2001. Genome of the bacterium *Streptococcus pneumoniae* strain R6. J Bacteriol. 183(19):5709-17.

Ilan O, Bloch Y, Frankel G, Ullrich H, Geider K, Rosenshine I. 1999. Protein tyrosine kinases in bacterial pathogens are associated with virulence and production of exopolysaccharide. EMBO J. 18(12):3241-8.

Jayaratne P, Keenleyside WJ, MacLachlan PR, Dodgson C, Whitfield C. 1993. Characterization of *rcsB* and *rcsC* from *Escherichia coli* O9:K30:H12 and examination of the role of the *rcs* regulatory system in expression of group I capsular polysaccharides. J Bacteriol. 175(17):5384-94.

Lai YC, Peng HL, Chang HY. 2003. RmpA2, an activator of capsule biosynthesis in *Klebsiella pneumoniae* CG43, regulates K2 cps gene expression at the transcriptional level. J Bacteriol. 185(3):788-800.

Mizuta K, Ohta M, Mori M, Hasegawa T, Nakashima I, Kato N. 1983. Virulence for mice of Klebsiella strains belonging to the O1 group: relationship to their capsular (K) types. Infect Immun. 40(1):56-61.

Nesper J, Hill CM, Paiment A, Harauz G, Beis K, Naismith JH, Whitfield C. 2003.

Translocation of group 1 capsular polysaccharide in *Escherichia coli* serotype K30. Structural and functional analysis of the outer membrane lipoprotein Wza. J Biol Chem. 278(50):49763-72.

Paiment A, Hocking J, Whitfield C. 2002. Impact of phosphorylation of specific residues in the tyrosine autokinase, Wzc, on its activity in assembly of group 1 capsules in *Escherichia coli*. J Bacteriol. 184(23):6437-47.

Paulsen, I.T., Beness, A.M., Saier, M.H. 1997. Computer-based analyses of the protein constituents of transport systems catalysing export of complex carbohydrates in bacteria. Microbiology 143: 2685-2699 Clin Microbiol Rev. 11(4):589-603

Pavelka MS Jr, Hayes SF, Silver RP. 1994 Characterization of KpsT, the ATP-binding component of the ABC-transporter involved with the export of capsular polysialic acid in *Escherichia coli* K1. J Biol Chem. 269(31):20149-58.

Podschun R, Ullmann U. 1998. *Klebsiella* spp. as nosocomial pathogens: epidemiology, taxonomy, typing methods, and pathogenicity factors. Clin Microbiol Rev. 11(4):589-603.

Preneta R, Jarraud S, Vincent C, Doublet P, Duclos B, Etienne J, Cozzone AJ. 2002. Isolation and characterization of a protein-tyrosine kinase and a phosphotyrosine-protein phosphatase from *Klebsiella pneumoniae*. Comparative Biochemistry and Physiology Part B 131103-112

Rahn A, Beis K, Naismith JH, Whitfield C. 2003. A novel outer membrane protein, Wzi, is involved in surface assembly of the *Escherichia coli* K30 group 1 capsule. J Bacteriol. 185(19):5882-90.

Reuhs BL, Geller DP, Kim JS, Fox JE, Kolli VS, Pueppke SG. 1998. *Sinorhizobium fredii* and *Sinorhizobium meliloti* produce structurally conserved lipopolysaccharides and strain-specific K antigens. Appl Environ Microbiol. 64(12):4930-8.

Russo TA, Wenderoth S, Carlino UB, Merrick JM, Lesse AJ. 1998. Identification, genomic organization, and analysis of the group III capsular polysaccharide genes *kpsD*, *kpsM*, *kpsT*, and *kpsE* from an extraintestinal isolate of *Escherichia coli* (CP9, O4/K54/H5). J Bacteriol. 180(2):338-49.

Simoons-Smit AM, Verweij-van Vught AM, MacLaren DM. 1986. The role of K antigens as virulence factors in *Klebsiella*. J Med Microbiol. Mar;21(2):133-7.

Stevenson G, Andrianopoulos K, Hobbs M, Reeves PR. 1996. Organization of the *Escherichia coli* K-12 gene cluster responsible for production of the extracellular polysaccharide colanic acid. J Bacteriol. 178(16):4885-93.

Stout V, Torres-Cabassa A, Maurizi MR, Gutnick D, Gottesman S. 1991. RcsA, an unstable positive regulator of capsular polysaccharide synthesis. J Bacteriol. 173(5):1738-47.

Stevenson, G., K. Andrianopoulos, M. Hobbs, and P. R. Reeves. 1996. Organization of the *Escherichia coli* K-12 gene cluster responsible for production of the extracellular polysaccharide colanic acid. J. Bacteriol. 178:4885-4893

Wacharotayankun R, Arakawa Y, Ohta M, Hasegawa T, Mori M, Horii T, Kato N. 1992. Involvement of *rcsB* in *Klebsiella* K2 capsule synthesis in *Escherichia coli* K-12. J Bacteriol. 174(3):1063-7.

Whitfield C, Perry MB, MacLean LL, Yu SH. 1992. Structural analysis of the O-antigen side chain polysaccharides in the lipopolysaccharides of *Klebsiella* serotypes O2(2a), O2(2a,2b), and O2(2a,2c). J Bacteriol. 174(15):4913-9.

Whitfield C, Roberts IS. 1999. Structure, assembly and regulation of expression of capsules in *Escherichia coli*. Mol Microbiol. 31(5):1307-19.

Wugeditsch T, Paiment A, Hocking J, Drummelsmith J, Forrester C, Whitfield C. 2001. Phosphorylation of Wzc, a tyrosine autokinase, is essential for assembly of

group 1 capsular polysaccharides in *Escherichia coli*. J Biol Chem. 276(4):2361-71.

Vincent C, Doublet P, Grangeasse C, Vaganay E, Cozzone AJ, Duclos B. 2000. Cells of *Escherichia coli* contain a protein-tyrosine kinase, Wzc, and a phosphotyrosine-protein phosphatase, Wzb. J Bacteriol. 181(11):3472-7.

Vodonik SA, Gray GR. 1988. Analysis of linkage positions in a polysaccharide containing nonreducing, terminal alpha-D-glucopyranosyluronic groups by the reductive-cleavage method. Carbohydr Res. 172(2):255-66.

Yoshida T, Ayabe Y, Yasunaga M, Usami Y, Habe H, Nojiri H, Omori T. 2003. Genes involved in the synthesis of the exopolysaccharide methanolan by the obligate methylotroph *Methylobacillus* sp strain 12S. Microbiology. 149(Part 2):431-44.

Table 1. Bacterial strains used and constructed in this study

Strain	Genotype or relevant property	Reference or source
E. coli:		
XL1-blue(DE3)	*recA endA1 gyrA96 thi-1 hsdR17 supE44 relA1 lac*[F' *pro AB* $lac^qZ\triangle$M15:: Tn*10*](DE3);Tet^r	Stratagene
NovaBlue(DE3)	*endA1 hsdR17*($rk_{12}^-mk_{12}^+$) *supE44 thi-1 recA1 gyrA96 relA1 lac*[F' *pro AB* $lac^qZ\triangle$M15:: Tn*10*](DE3);Tet^r	Novagen
JM109	*RecA1 supE44 endA1 hsdR17 gyrA96 rolA1 thi* △ *(lac-proAB)*	Laboratory stock
BL21-RIL	F^- *ompT hsdS*$_B$($r_B^-m_B^-$)*gal dcm*(DE3)	Laboratory stock
S17-1λ*pir*	Tp^r Sm^r *recA, thi, pro, hsdR*$^-M^+$ [RP4-2-Tc::Mu:Km^rTn*7*] (*pir*)	De Lorenzo *et al.*, 1994
ICC188λ*pir*	△*(ara-leu) araD* △*lac×74 galE galK phoA20*	Taylor *et al.*,1989
K. pneumoniae:		
CG43	Clinical isolate of K2 serotype	Laboratory stock
CG43-S3	*rspl* mutant, $Strep^r$	Laboratory stock
CG43-S3-U9451	*galU* deletion mutant	Laboratory stock
CG43-S3-*yor5*$^-$	*yor5* deletion mutant in CG43-S3	This study
CG43-S3-*yco6*$^-$	*yco6* deletion mutant in CG43-S3	This study
CG43-S3-*wzx*$^-$	*wzx* deletion mutant in CG43-S3	This study
CG43-S3-*wza*$^-$	*wza* deletion mutant in CG43-S3	This study

Table 2. Plasmids used and constructed in this study

Plasmids	Relevant characteristic	Source or reference
pGEM-Teasy	PCR cloning vector, Ap^r	Promega
YT&A vector	PCR cloning vector, Ap^r	Yeastern Biotech
pET-30a	Expression vector, Km^r	Novagene
pET-30b	Expression vector, Km^r	Novagene
pET-30c	Expression vector, Km^r	Novagene
pKAS46	Suicide vector, Ap^r Km^r	Laboratory stock
pRK415	Shuttle vector, *mob*$^+$, Tc^r	This study
pYor5	A 0.8-kb fragment of *yor5* cloned into pGEM-T vector, Ap^r	This study
pYco6E22	A 0.8-kb fragment of C-terminal *yco6* ($Yco6^{435-707}$)cloned into pGEM-T vector, Ap^r	This study
pYco6E23	A 1.0-kb fragment of C-terminal *yco6* ($Yco6^{435-722}$)cloned into pGEM-T vector, Ap^r	This study
pWzx	A 1.5-kb fragment of *wzx* cloned into Y&T vector, Ap^r	This study
pWza	A 1.1-kb fragment of *wza* cloned into Y&T vector, Ap^r	This study
pORF1	A 0.9-kb fragment of *orf1* cloned into Y&T vector, Ap^r	This study
pORF3	A 1.4-kb fragment of *orf3* cloned into Y&T vector, Ap^r	This study
pORF15	A 1.4-kb fragment of *orf15* cloned into Y&T vector, Ap^r	This study
pUGD	A 1.2-kb fragment of *ugd* cloned into Y&T vector, Ap^r	This study
pET-Yor5	pET30b-derivative expressing Yor5-His_6-tag fusion: Yor5 was cloned on a *Eco*R Ⅴ/*Sac* Ⅰ fragment, Km^r	This study
pET-Yco6E22	pET30b-derivative expressing $Yco6^{435-707}$ -His_6-tag fusion into *Eco*R Ⅴ/*Sac* Ⅰ site	This study
pET-Yco6E23	pET30b-derivative expressing $Yco6^{435-722}$ -His_6-tag fusion into *Eco*R Ⅴ/*Sac* Ⅰ site	This study
pET-ORF1	pET30c-derivative expressing ORF1-His_6-tag fusion: ORF1 was cloned on a *Bam*H Ⅰ/*Hind* Ⅲ fragment, Km^r	This study
pET-ORF3	pET100-derivative expressing ORF3-His_6-tag fusion	This study
pET-ORF4	pET30c-derivative expressing ORF4-His_6-tag fusion cloned into a *Bam*H Ⅰ/*Hind* Ⅲ site	This study
pET-ORF15	pET30a-derivative expressing ORF15-His_6-tag fusion cloned into a *Bam*H Ⅰ/ *Sac* Ⅰ site	This study
pET-UGD	pET30c-derivative expressing ORF4-His_6-tag fusion: ORF4 was cloned on a *Eco*R Ⅰ/*Sal* Ⅰ fragment, Km^r	This study

Deletion clones		
pASm5	A 2.0-kb fragment containing a 150-bp deletion in *yor5* locus cloned into pKAS46, Ap^r Km^r	This study
pASm6	A 2.0-kb fragment containing a 1800-bp deletion in *yoc6* locus cloned into pKAS46, Ap^r Km^r	This study
pASma	A 2.0-kb fragment containing a 500-bp deletion in *wza* locus cloned into pKAS46, Ap^r Km^r	This study
pASmw	A 2.0-kb fragment containing a 600-bp deletion in *wzx* locus cloned into pKAS46, Ap^r Km^r	This study

Table 3. Primers used in this study

Primer	Sequence
Yor4	5’-CTCCATTGGTTCGTTGGAAT-3’
Yor3	5’-GCATTCGCTTGTTTCTGTTC-3’
Y5D1	5’-GGTTGGCGATATCTTAATGG-3’
Y5D2	5’-GCTGATTGGTGAGCTCCATG-3’
Y5D3	5’-CGAAGCACGAGCTCAGACA-3’
Y5D4	5’-AATCGCTCCGGACCATTGGC-3’
Y6E1	5’-AGAAATTCAGGATATCATGCATG-3’
Y6E2	5’-TGGCCTTGTGATATCAGTAAGCC-3’
Y6E3	5’-CACACCATTCAGAAAACATCC-3’
Y6E4	5’-AAGGGGATTCTTCGTCCCCT-3’
Y6D1	5’-AGAGGGATATCAAATAAGCGTGT-3’
Y6D2	5’-CCACACCATTCAGGATCCATCCT-3’
Y6D3	5’-ATAGGATCCTCAAGAAGGGGACG-3’
Y6D4	5’-TATTAGATGCGAGCTCACGGC-3’
WxE1	5’-GATGAGTTTAAAATTAAAAACGATAA-3’
WxE2	5’-GAATGATTTGGCAGCATATTTA-3’
WxD1	5’-TCGATATCGCTATATTGACAACC-3’
WxD2	5’-AGAAAGCTTAATCTATCCAGCC-3’
WxD3	5’-CTGCAAAGCTTGGTTTATGCA-3’
WxD4	5’-CTGATAGATGAGCTCTGGAATG-3’
WaE1	5’-CACC AAGAAAAAAATTGTTAGATTTTCG-3’
WaE2	5’-CTAAACATATTATGGCCAATCC-3’
WaD1	5’-TTTCTATGGGCAGATGGTTG-3’
WaD2	5’-CAGAATTCACCCAGTTACCG-3’
WaD3	5’-CCGCAGTGGTATGACAATTG-3’
WaD4	5’-GCTGACTATCGGGAAGCATC-3’
ORF1E1	5’-TTGCAACCAAACAGGTGAAG-3’
ORF1E2	5’-GGTTTCAGGCTGGCGCTCA-3’
ORF3E1	5’-CACC ATAAAAATTGCGCGCATTG-3’
ORF3E2	5’-CCCTTATTTTCAGCATTCAGC-3’
ORF15E1	5’-GACCACACCAGACAGGAGCAAGT-3’
ORF15E2	5’-CTCGGGCGGCATATAAAGA-3’
UGDE1	5’-CGAATGAAAATTACTATTTCCGG-3’
UGDE2	5’-CCAGTGTCAGACAGGCAGAA-3’

Table 4. Homology search analyses of the CPS gene cluster in *K. pneumoniae*.

	K2, strain Chedid	MCG 78578 (http://genome.nhri.org.tw)	Taiwan, NTUH-K2044 (http://genome.wustl.edu)
ORF1	**UTP-glucose-1-phosphate uridylyltransferase**	**UTP-glucose-1-phosphate uridylyltransferase**	**UTP-glucose-1-phosphate uridylyltransferase**
ORF2	**ORF2**	**ORF2**	**ORF2**
ORF3	**OrfX**	**OrfX**	**OrfX**
ORF4	**Wza**	**Wza**	**Wza**
ORF5	**Yor5**	**Yor5**	**Yor5**
ORF6	**Yco6**	**Yco6**	**Yco6**
ORF7	glycosyltransferase	undecaprenolphosphate gal-1-P transferase	**flippase, wzx**
ORF8	glycosyltransferase	rhamnosyl transferase	hypothetical protein
ORF9	mannosyl transferase	glycosyl transferase	mucoviscosity-associated protein A
ORF10	CapD	polysaccharide biosynthesis protein	hypothetical protein putative glycosyl transferase
ORF11	**flippase, Wzx**	putative glycosyl transferase	GDP-mannose 4,6-dehydratase
ORF12	hypothetical 65.4 kDa protein in CPS region	glycosyltransferase	GDP-mannose-4-keto-6-D epimerase
ORF13	acetyltransferase	Wzy	GDP-mannose mannosyl hydrolase
ORF14	sugar transferases	predicated ORF	putative colanic biosynthesis glycosyl transferase
ORF15	**6-phosphogluconate dehydrogenase**	predicted acyltransferases	putative colanic acid UDP-glucose lipid carrier
ORF16	mannose-1-phosphate guanylyltransferase	**flippase,Wzx**	**6-phosphogluconate dehydrogenase**
ORF17	phosphormannonutase dehydrogenase	**6-phosphogluconate dehydrogenase**	GDP-mannose pyrophosphorylase(manC)
ORF18	putative transport protein	dTDP-glucose 4,6-dehydratase	phosphomannomutase(manB)
ORF19	putative transport protein	glucose-1-phosphate thymidylyltransferase	UDP-glucose 6-dehydrogenase(ugd)
		dTDP-6-deoxy-L-mannose-dehydrogenase	putative nucleotide sugar epim9erase(wbnF)
		dTDP-6-deoxy-D-glucose -3,5-epimerase	
		rhamnosyl transferase	

The black frames represent the conserved genes in the three *K. pneumoniae* strains.

Table 5. Features of the ORFs encoded in K2 *cps* region from *k. pneumoniae*.

ORF	Signal peptide predicated	Putative transmembrane regions	Putative function	Organism (name of protein)	% identity/ % similarity	Accession no
Orf1	N	1	UTP-glucose-1-phosphate uridylyltransferase	*E. coli* (GalF)	99/98	AAN52283
Orf2	Y	6	unknown	*E. coli* (COG0671)	85/87	ZP_00272700
Orf3	Y	1	unknown	*E. coli* (OrfX)	97/99	AAD21561
Orf4	Y	1	putative outer membrane lipoprotein	*E. coli* (Wza)	91/96	AAD21562
Orf5	N	0	protein-tyrosine-phosphatase	*E. coli* (Wzb)	67/85	AAD29991
Orf6	N	2	tyrosine-protein kinase	*E. coli* (Wzc)	64/79	AAD21564
Orf7	N	1	glycosyltransferase	*P. fluorescens* (COG0438)	36/54	ZP_00263750
Orf8	N	0	glycosyltransferase	*B. japonicum* (bll2376)	31/51	ZP_00127611
Orf9	N	0	mannosyltransferase	*A. actinomycetemcomitans* (orf6)	35/53	BAA94398
Orf10	N	10	unknown	*A. actinomycetemcomitans* (orf5)	24/42	BAA94397
Orf11	N	12	flippase	*S. typhimurium* (Wzx)	47/67	AAG24819
Orf12	Y	3	unknown	*K. pneumoniae* (orf12)	97/97	Q48458
Orf13	N	0	acetyltransferase	*S. pneumoniae* (cps9vM)	30/48	AAM62297
Orf14	N	4	sugar transferases	*K. pneumoniae* (RfbP)	95/95	C56146
Orf15	N	1	6-phosphogluconate dehydrogenase	*E. coli* (Gnd)	98/98	I84555
Orf16	N	0	mannose-1-phosphate guanylyltransferase	*E. coli*	97/97	I57096
Orf17	N	0	phosphormannonutase dehydrogenase	*E. coli* (RfbK)	98/99	BAA07746
Orf18	N	4	putative transport protein	*S. flexneri* (YegH)	77/83	NP_837683

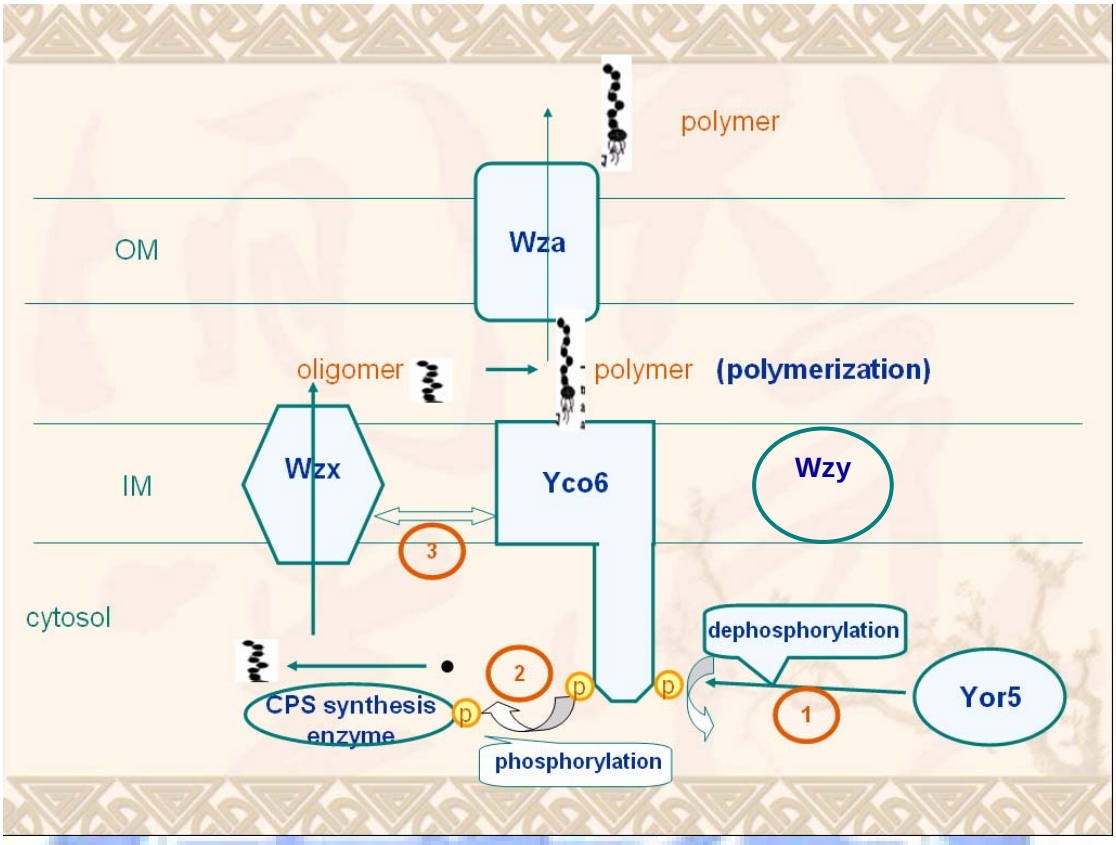

Fig. 1. Schematic illustration of the functional roles of the CPS core components. (1) Yor5 regulates the phosphorylation level of Yco6. (2) Yco6 phosphorylates the CPS synthesis enzymes to affect CPS production. (3)Yor5 affects CPS polymerization by regulates the interaction of Yco6 and Wzx.

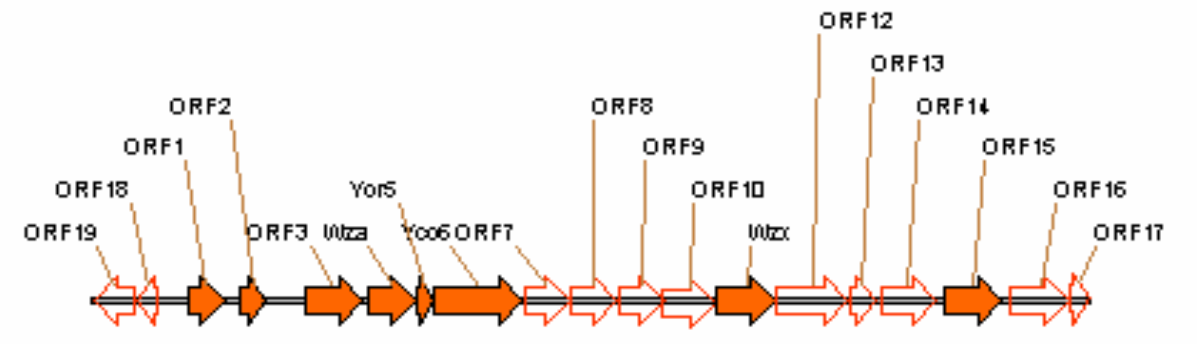

K2 strain Chedid, Japan

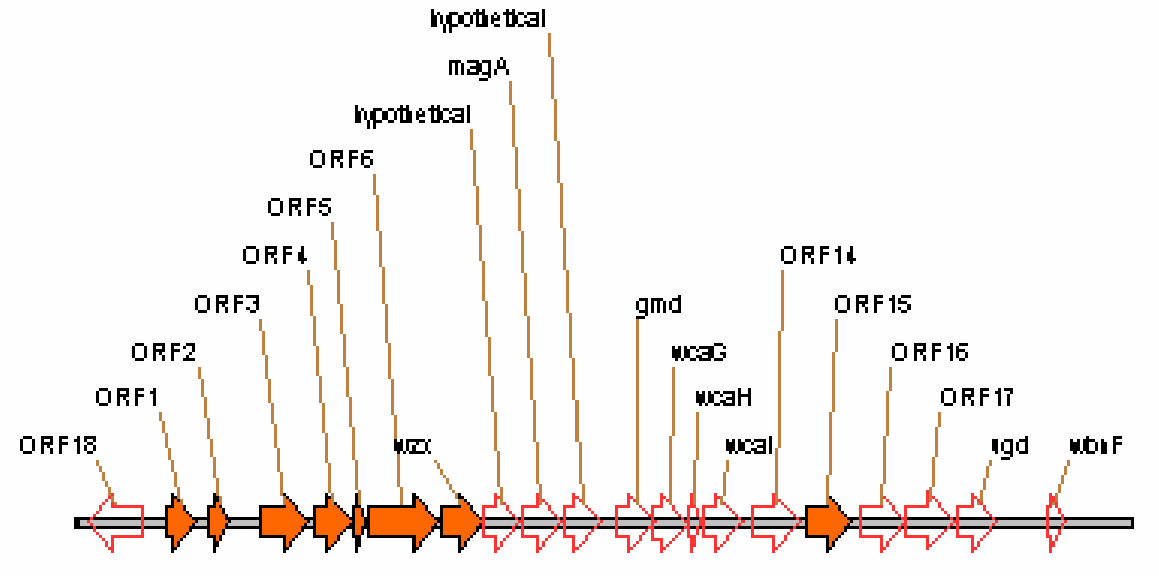

NTUH-K2044, Taiwan

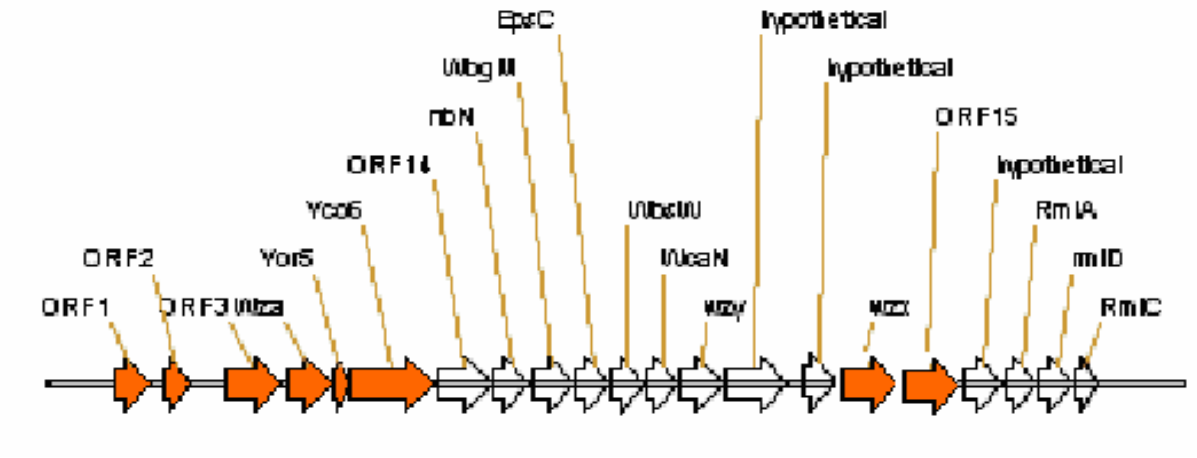

MCG 78578, Washington

Fig. 2. Comparative analysis of the *K. pneumoniae cps* gene clusters. The solid frames represent the conserved components in the three strains.

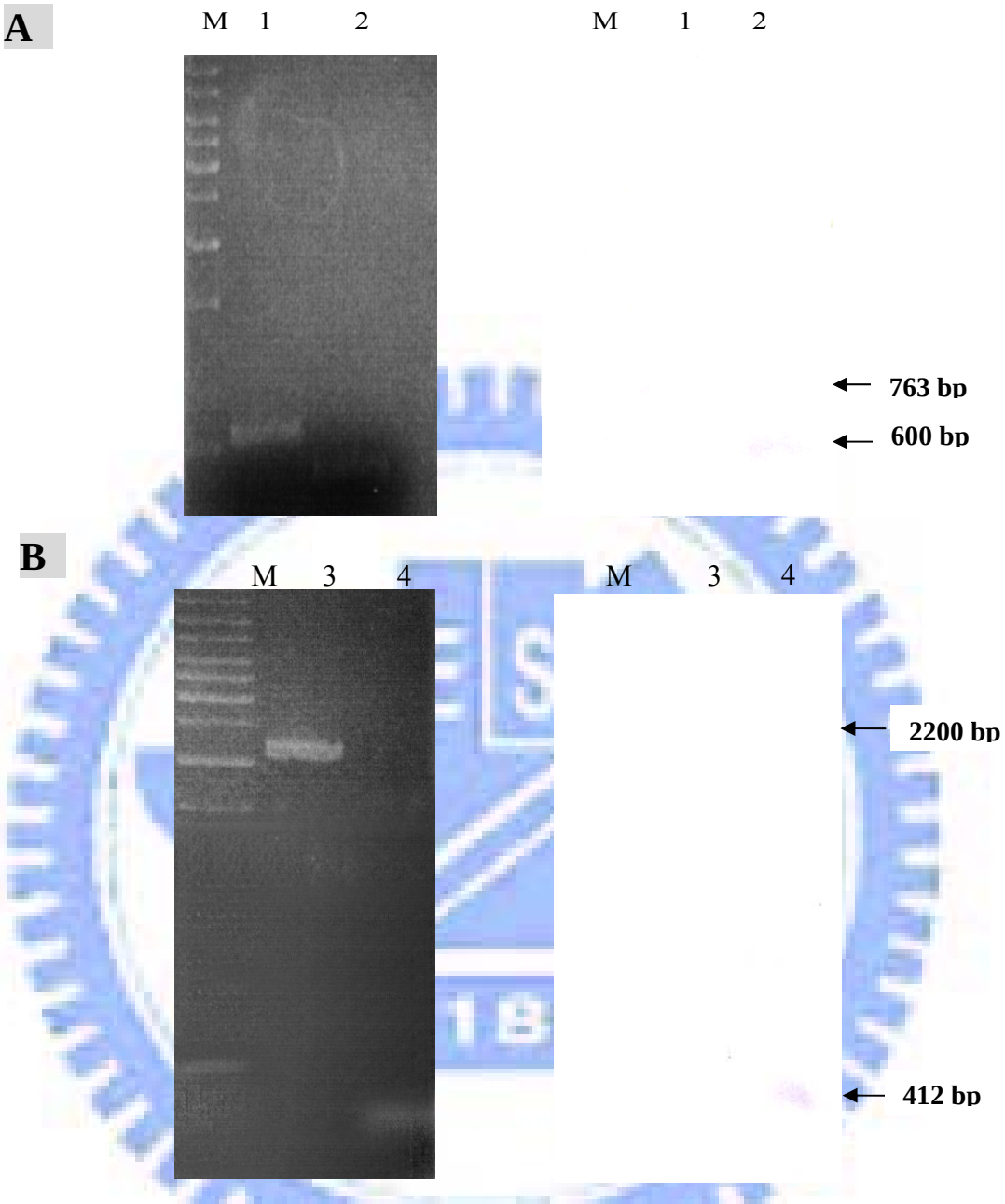

Fig. 3. Identification of *yor5* (A) and *yco6* (B) mutation by Southern blot analysis. The arrows represent the PCR products. Left panel, photographs of an ethidium bromide-stained agarose gel. Lanes M: DNA maker; 1: PCR product using primer pair yor3 and yor4 in *K. pneumoniae* CG43-S3, 2: PCR product using primer pair yor3 and yor4 in *K. pneumoniae* CG43-S3-*yor5*$^-$, 3: PCR product using primer pair yco6E1 and yco6E3 in *K. pneumoniae* CG43-S3, 4: PCR product using primer pair yco6E1and yco6E3 in *K. pneumoniae* CG43-S3-*yco6*$^-$. Right panels, Southern blot analysis using probes from coding regions of *yor5* and *yco6*, respectively.

A

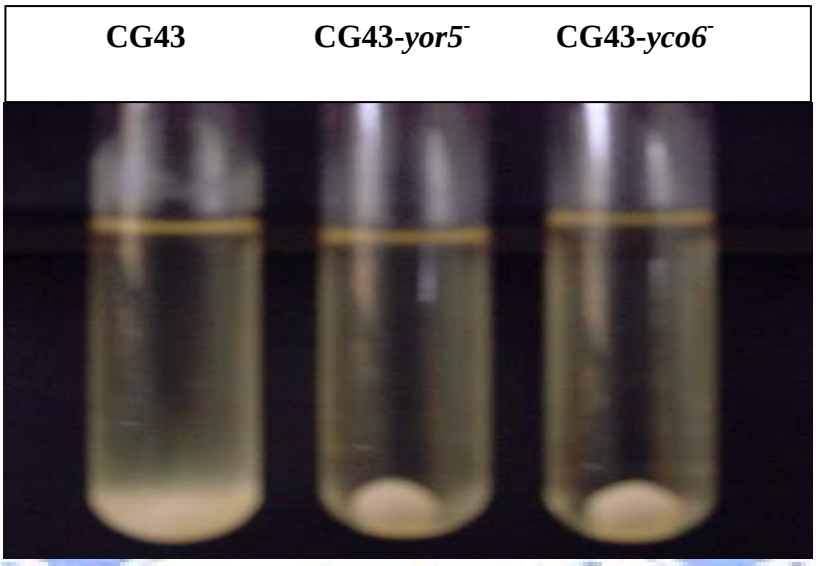

B

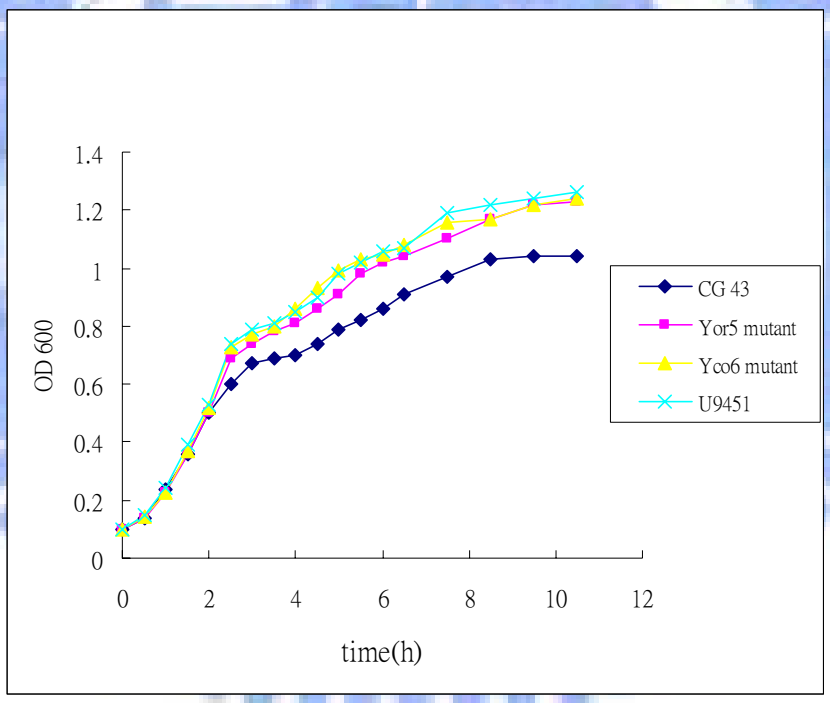

Fig. 4. Phenotype analysis of CG43, CG43-*yor5*⁻ and CG43-*yco6*⁻. U9451, a *galU* mutant, is used as a negative control because *galU* encodes the enzyme UDP-glucose pyrophosphorylase that regulates the supply of UDP-galactose and UDP-glucose, two major precursors for the biosynthesis of CPS (Chang et al., 1996) (A) Overnight culture of wild type strain CG43S3, CG43-*yor5*⁻ and CG43-*yco6*⁻ were subjected to 5000 g centrifugation for 5 min. (B) Growth curves of the bcteria CG43, CG43-*yor5*⁻, CG43-*yco6*⁻ and U9451 at 37 ℃ in LB broth.

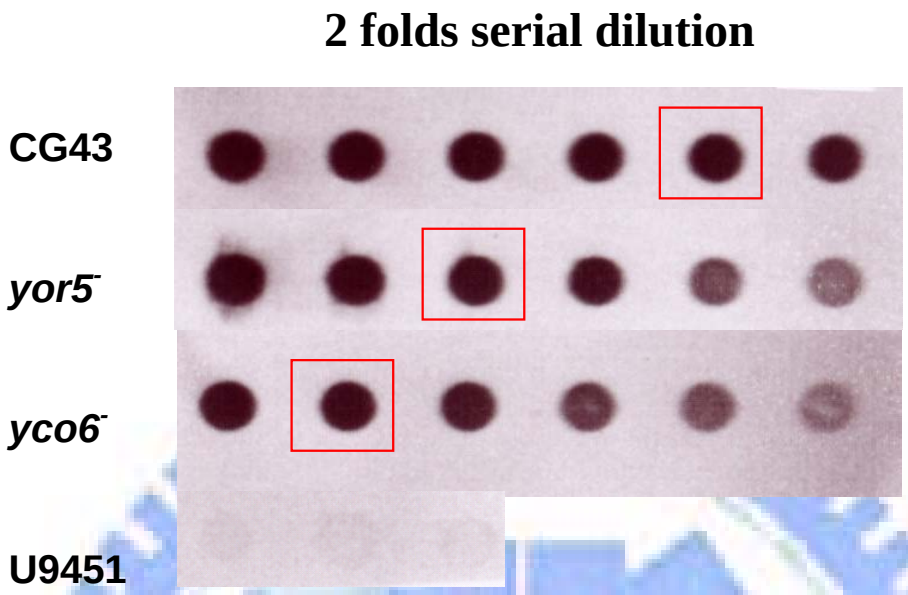

Fig. 5. Comparison of CPS production of CG43-S3, CG43-S3-*yor5*$^-$, CG43-S3-*yco6*$^-$, and U9451. The CPS were extracted with hot-phenol and treated with protease K, appeared to be measured and probed with K2 antiserum. The frames represent equal amount of CPS analyzed with ScanAlyze (Michael Eisen , Stanford University).

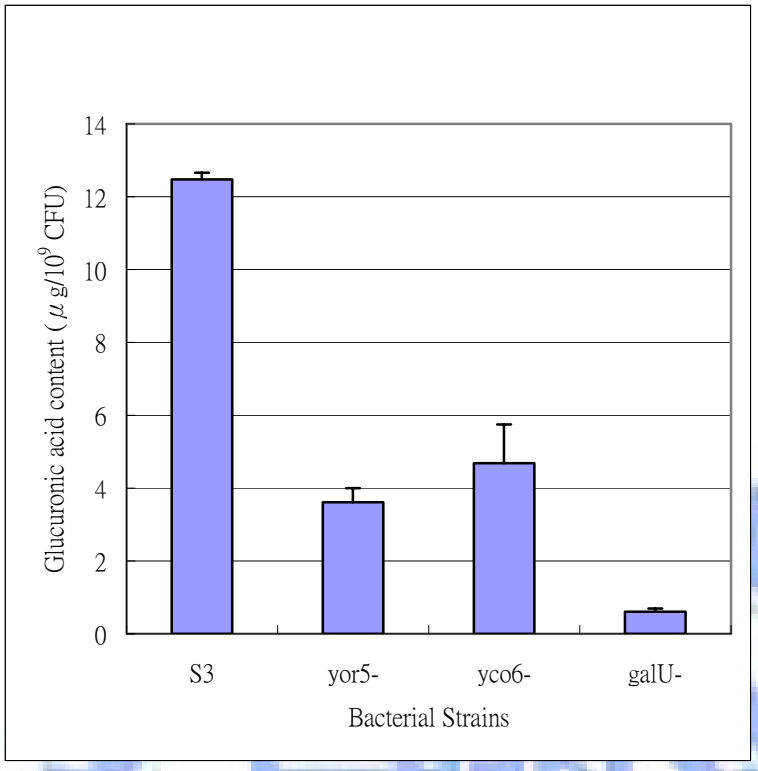

Fig. 6. Glucuronic acid contents of CG43, CG43-*yor5*$^-$, CG43-*yco6*$^-$ and U9451. CPS of the bacteria from 500 µl of overnight culture was extracted and then hydrolyzed by H_2SO_4, and then 3-hydroxydiphenol was added to measure the absorbance at 520 nm. Glucuronic acid was used as standard for the quantification of uronic acid.

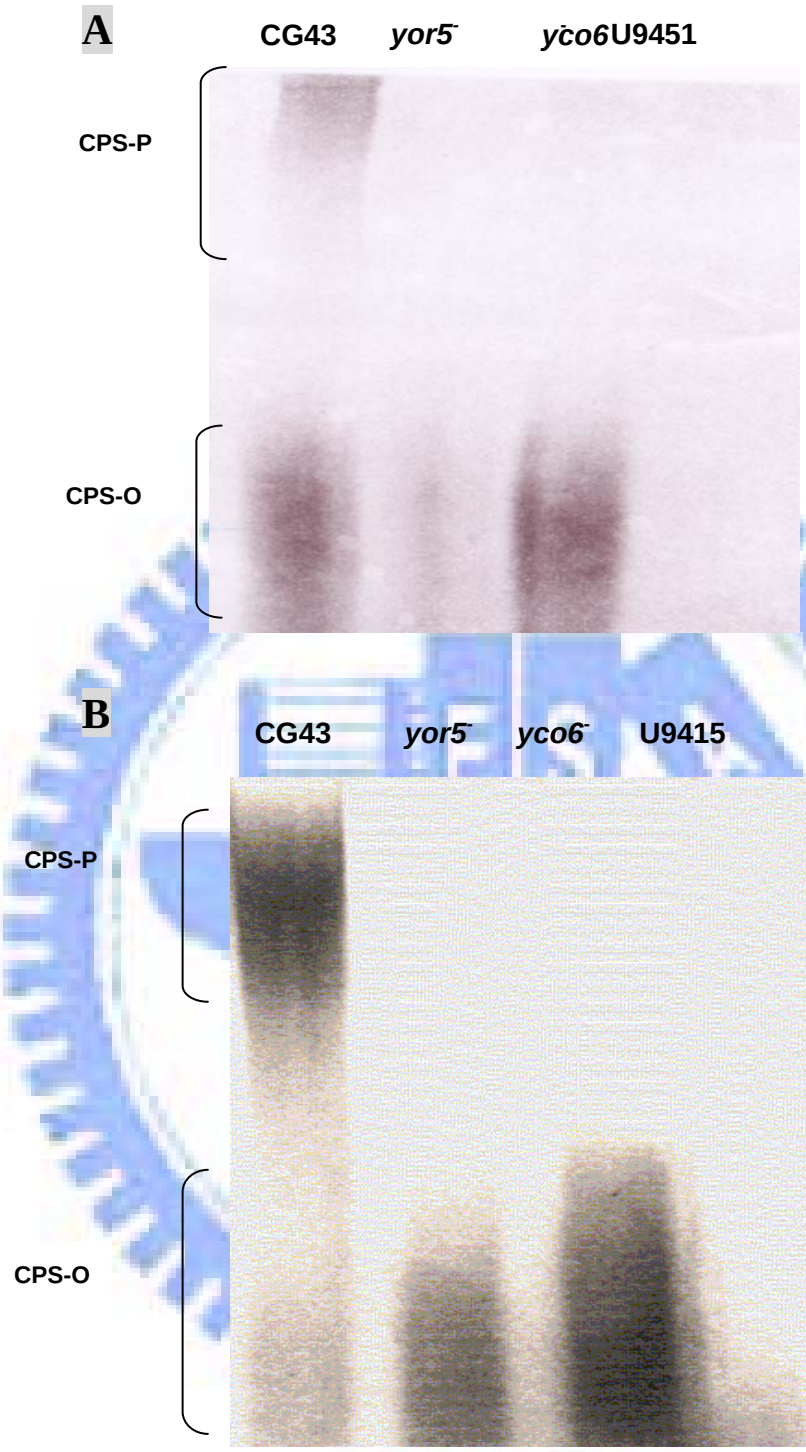

Fig. 7. Both Yor5 and Yco6 affected the polymeric CPS production. The CPS was extracted with hot-phenol, treated with protease K and analyzed with 5% DOC PAGE. Panel A shows immune blot analysis probed with polyclonal K2 antiserum. Panel B shows the alcian blue-silver stained DOC PAGE. CPS-P represents high molecular weight polymeric CPS. CPS-O represents low molecular weight oligomeric CPS.

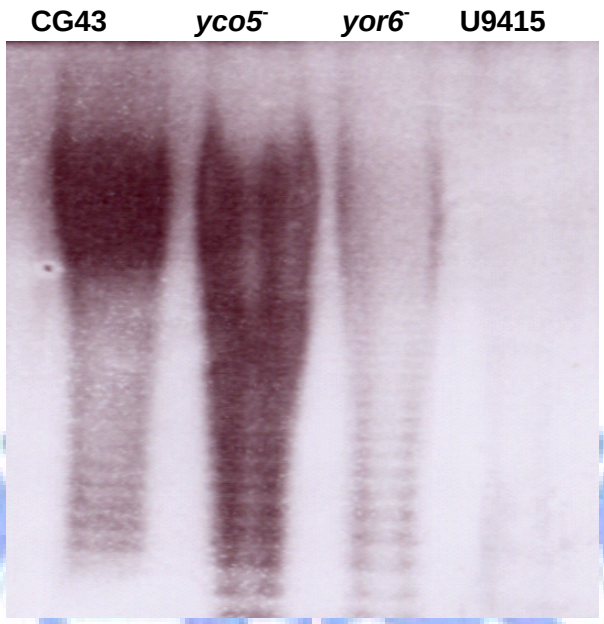

Fig. 8. Neither *yor5* nor *yco6* mutation affected the oligomeric CPS synthesis. The CPS were extracted with hot-phenol and treated with protease K and the CPS analyzed with alcian blue-silver stained 10% DOC PAGE. Alcian blue is a cationic dye and capable of binding to negative CPS to increase the sensitivity in CPS detection.

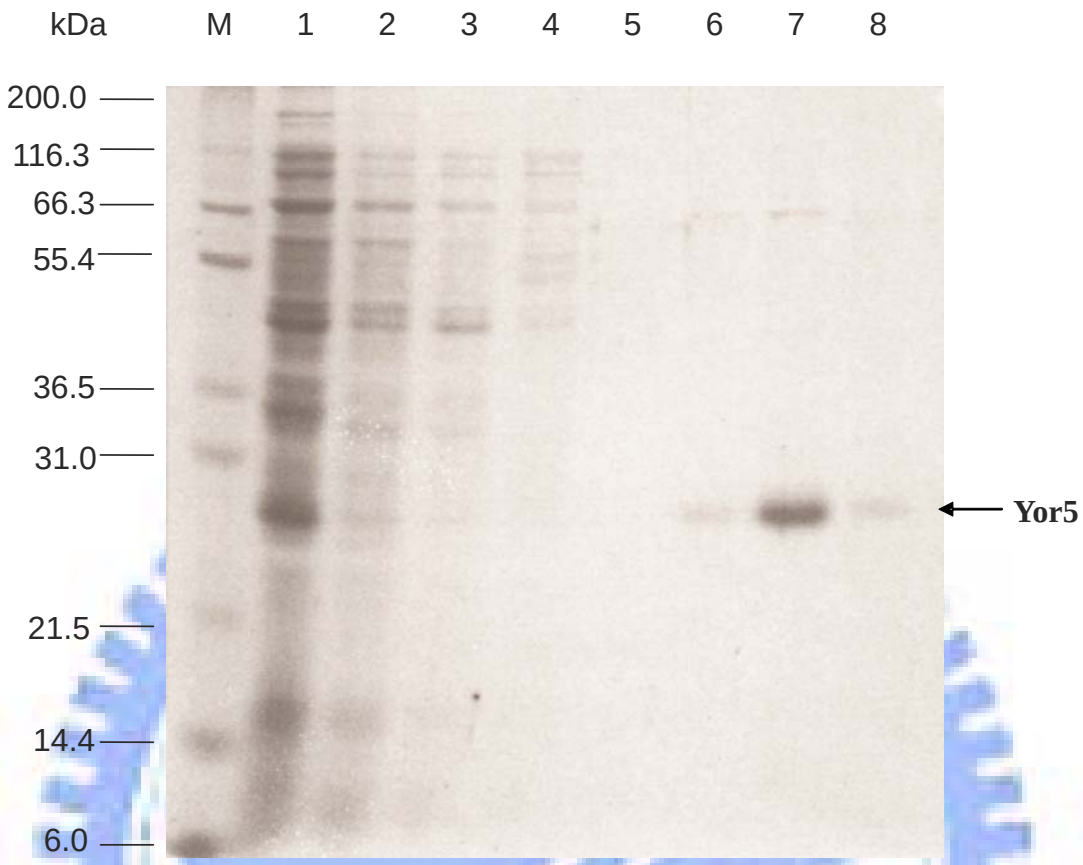

Fig. 9 Purification of the His_6-Yor5 recombinant protein. The His_6-Yor5 was overexpressed in *E. coli* NovaBlue (DE3) and purified through Ni^{+2} affinity column. The purified proteins were resolved by 12.5% SDS PAGE and then stained with Coomassie blue. Lane 1, protein molecular weight marker; lane 2, the whole cell lysate; lane 3, soluble proteins; lane 4, binding buffer elution； lane 5:washing buffer elution; lane 6 to lane 8, the purified fractions.

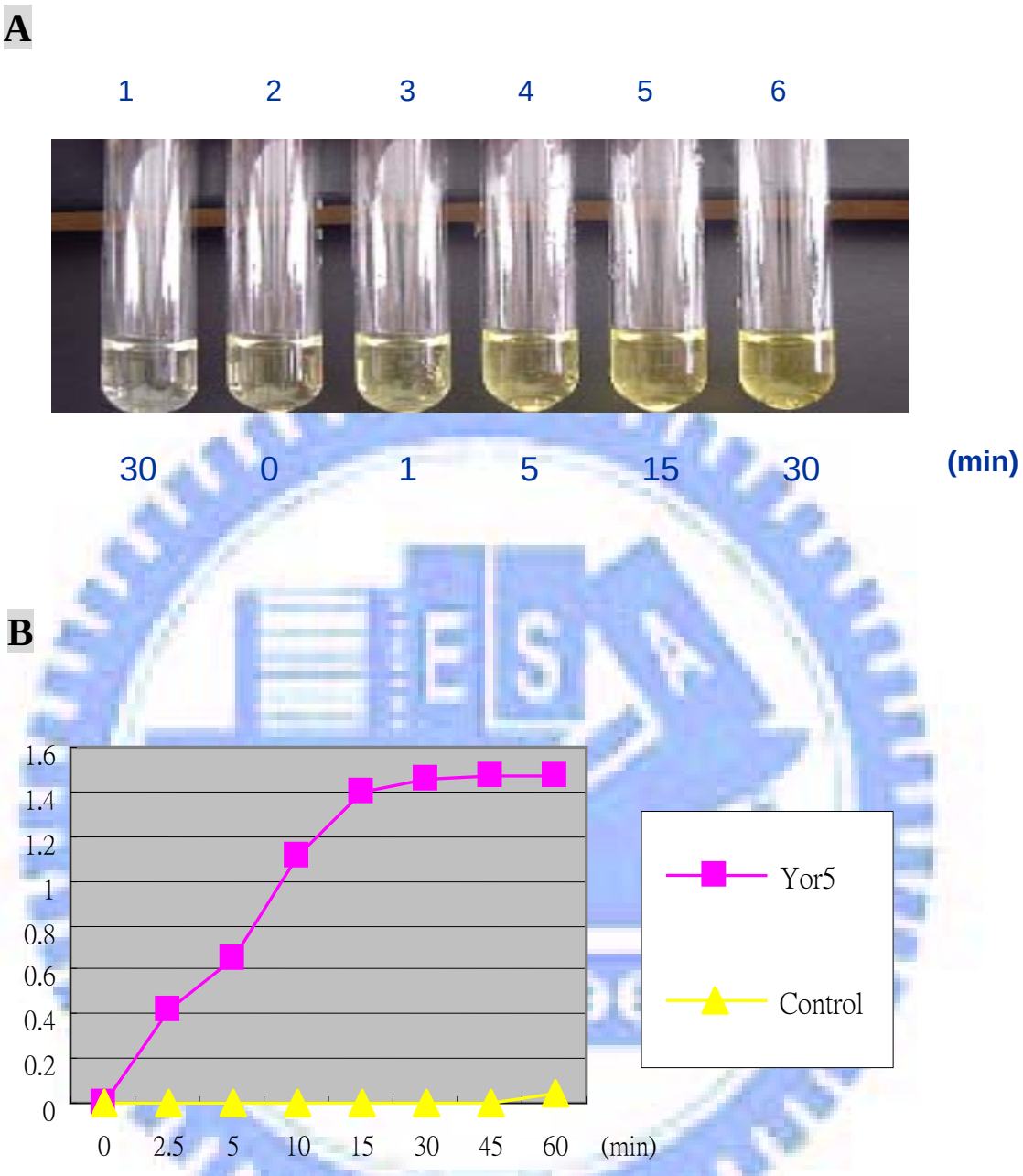

Fig. 10. Assessment of the phosphatase activity of the recombinant Yor5. The phosphatase activity of Yor5 was determinated by measurement of the decomposition of Para-nitrophenyl phosphate (pNPP) at 37 ℃ (A). Tube 1 to 5 each contained 4 μg/ml Yor5 in PNPP reaction buffer. Tube 6 is the blank containing only the PNPP reaction buffer. The phosphatase activity of Yor5 with PNPP as the substrate is 3.2×10^{-7} moles/min/mg (B).

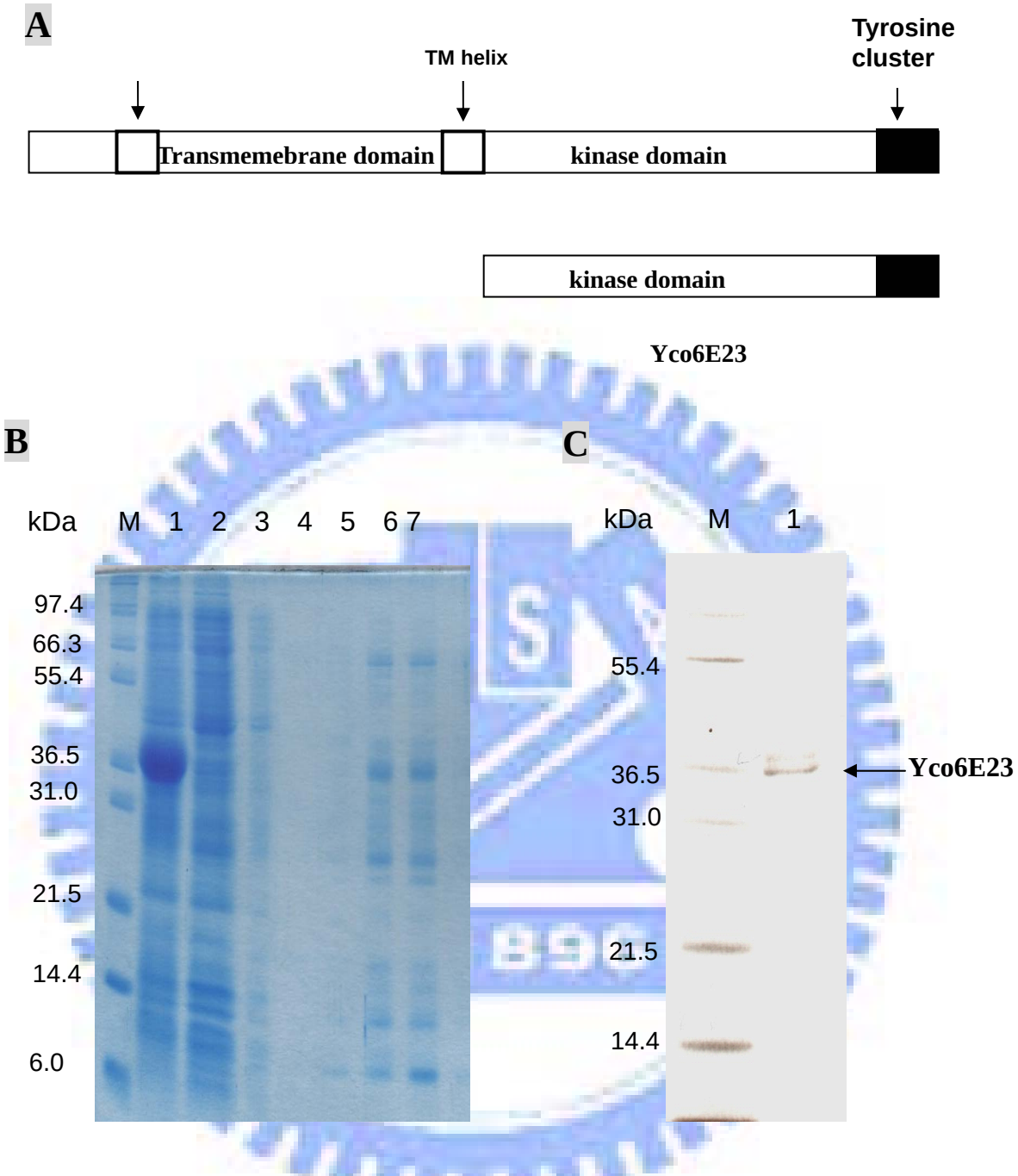

Fig. 11. Purification of the His_6-Yco6E23 recombinant protein. Panel A: Yco6E23 is a truncated form of Yco6 Panel B His_6-Yco6E23 was overexpressed in *E. coli* and purified by Ni^{+2} affinity column and resolved on 12.5% SDS PAGE using Coomassie Blue-staining. M, protein marker; lane 1, total protein; lane 2, soluble proteins; lane 3, binding buffer elution; lane 4: washing buffer elution; lanes 5 to 7, the eluted fractions. Panel C: Purification of the His_6-Yco6E23 recombinant protein by raising the imidazole concentration of wash buffer to 125 mM, M: protein maker; Lane 1: is the purified recombinant protein Yco6E23.

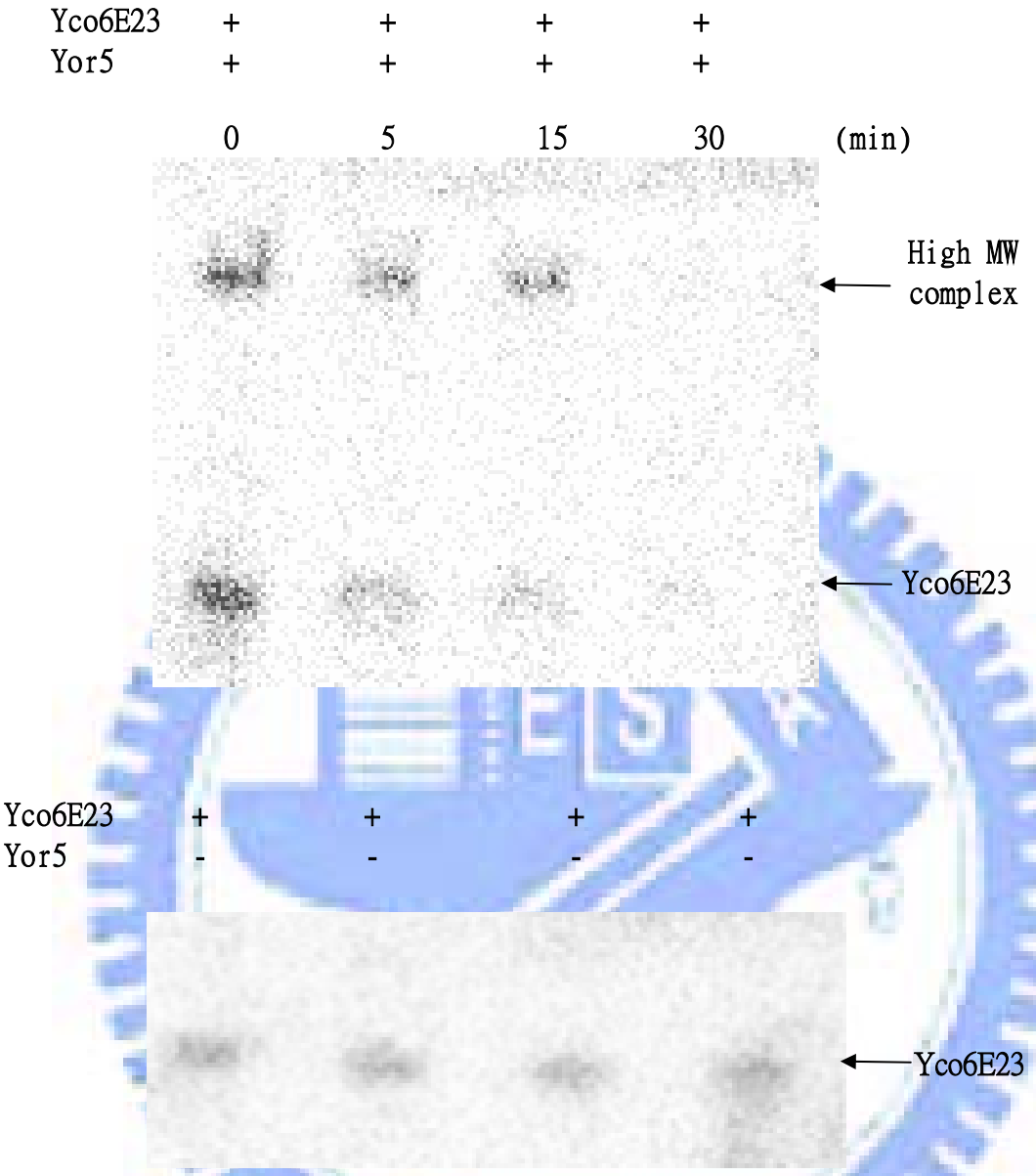

Fig. 12. In vitro dephosphorylation assay. The reaction mixes were separated with 12.5 % SDS PAGE, and the radioactive proteins were visualiz by InstantImager™ (Packard Instrument Company).

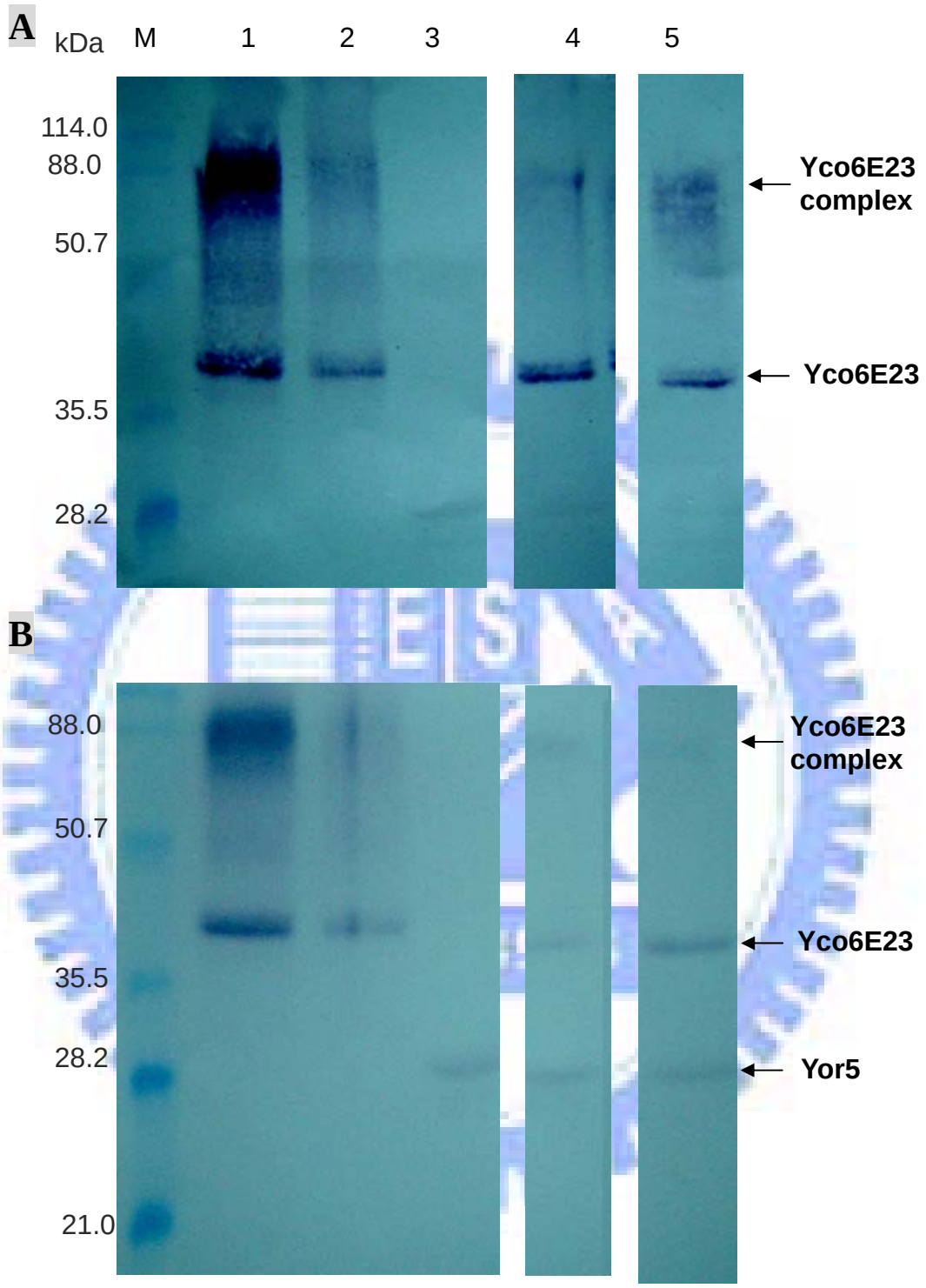

Fig. 13. Identification of Yco6E23 complex. The protein samples were separated with 12.5% SDS PAGE. The Western blot probed with anti-phosphotyrosine monoclonal antibody (Sigma P3300) was shown in panel A. Panel B represents the blot probed with anti-His tag monoclonal antibody (Novagen). M, protein maker; lane 1, Yco6E23: lane 2, Yco6E23 (100 ℃); lane 3, Yor5; lane 4, Yco6E23+Yor5; lane 5 (100 ℃)

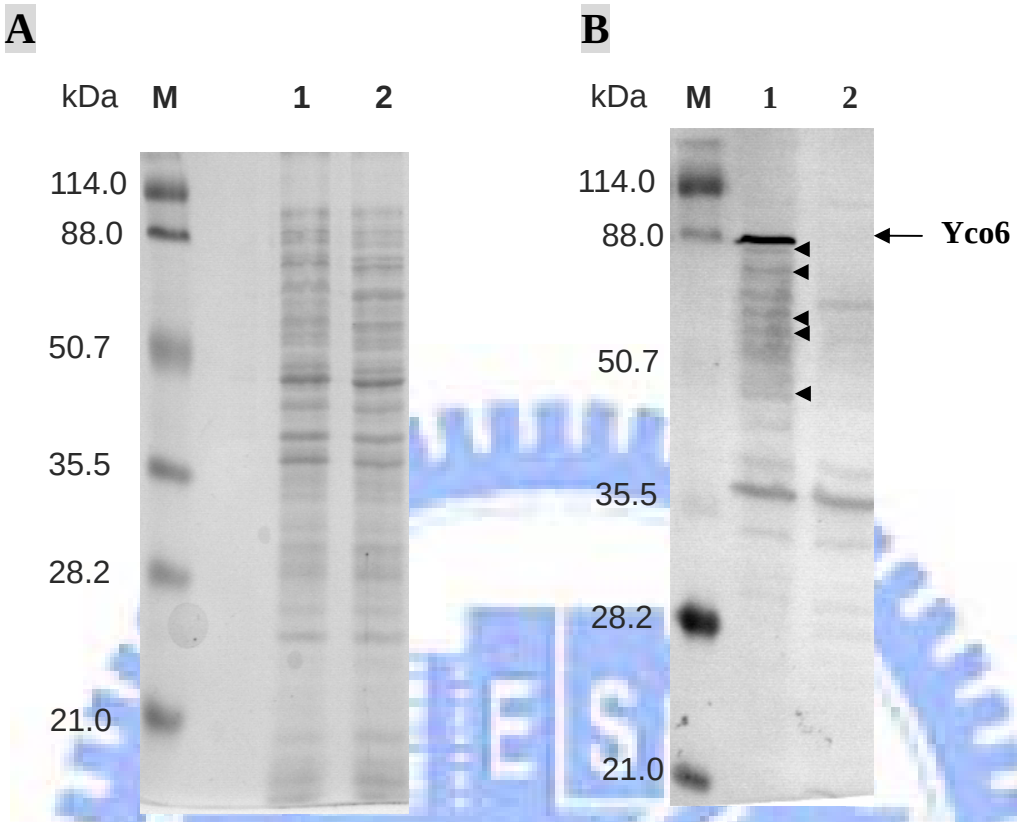

Fig. 14. Comparsion of the phosphotyrosine proteins between wild type and CG43-S3-*yco6*$^{-}$. Panel A shows Coomassie Blue-stained SDS-PAGE; Panel B shows the corresponding Western blot probed with monoclonal anti-phosphotyrosine antibody (Sigma P3300). M, protein maker; lane 1, CG43-S3 whole cell lysate; lane 2, CG43-S3-*yco6*$^{-}$ whole cell lysate; The arrows (▶) represent probable targets of Yco6 and the arrow (⟶) represents Yco6.

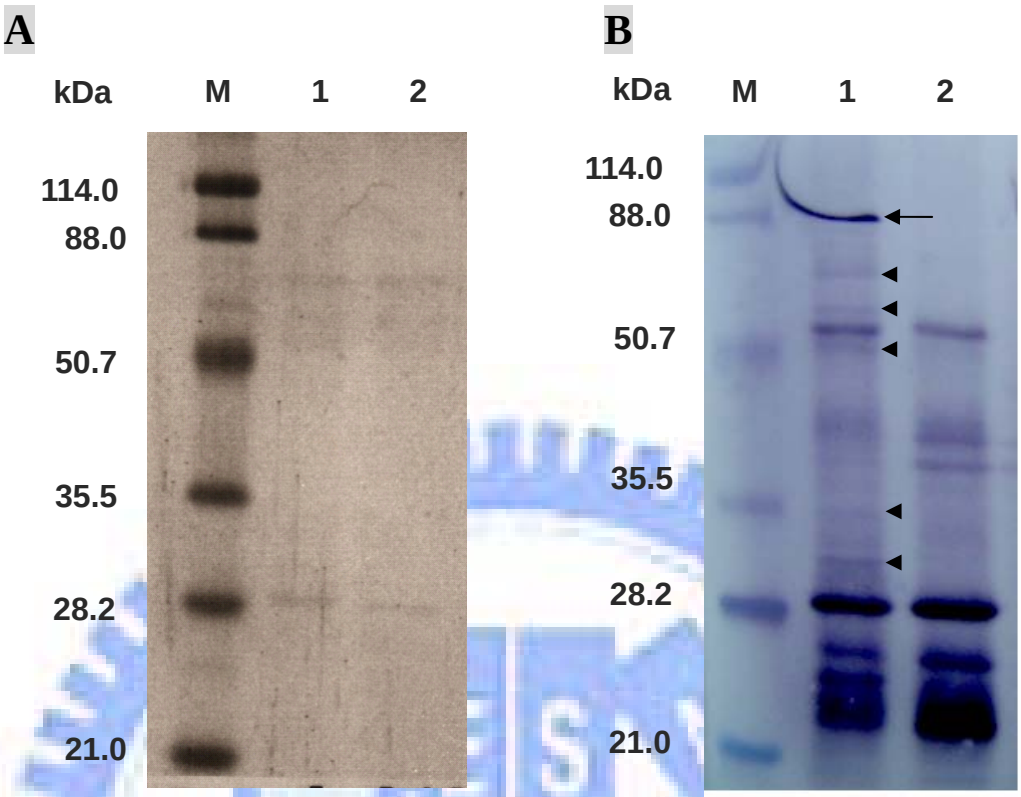

Fig. 15. The Yco6-interacting proteins identified using immunoprecipitation. Immunoprecipitation was used with monoclonal anti-phosphotyrosine antibody (Sigma PT66) from the whole cell protein. Then the protein-antibody complex was cached by proteinA/G. Panel A shows Coomassie Blue-stained SDS PAGE; Panel B shows corresponding Western blot probed with monoclonal anti-phosphotyrosine antibody (Sigma P3300). M, protein maker; lane 1, CG43-S3; lane 2, CG43-S3-*yco6*$^{-}$. The arrows (►) represent probable targets of Yco6 and the arrow (⟶) represents Yco6.

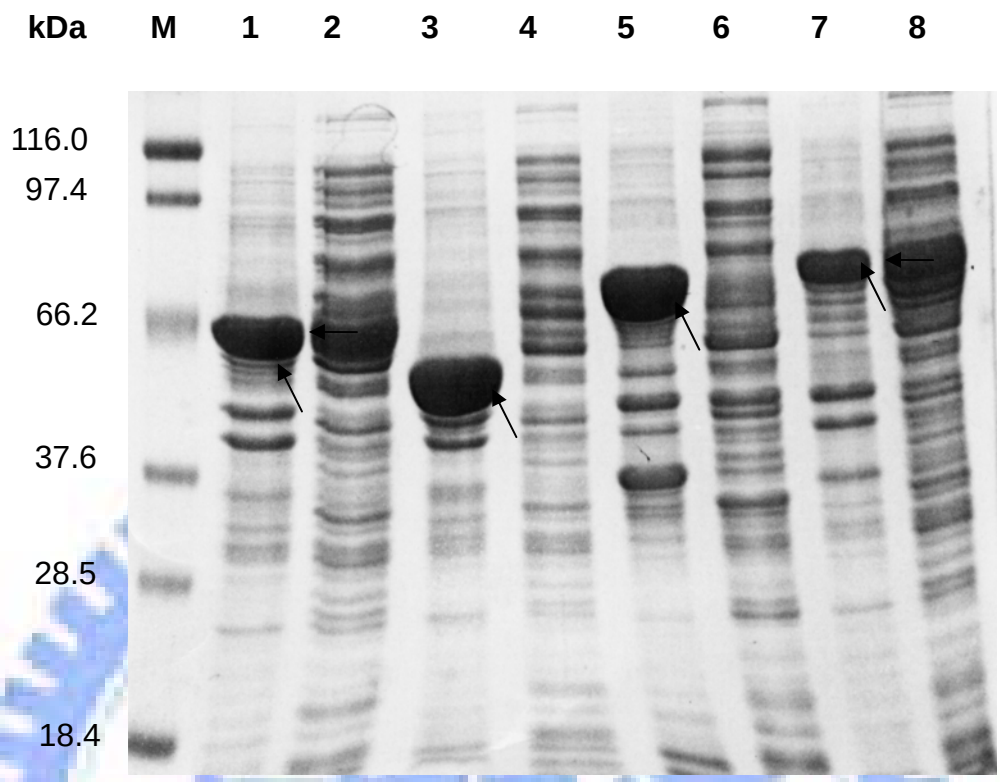

Fig. 16. Overexpression of *ugd, orf1, orf3* and *orf15* in *E. coli* NovaBlue (DE3). The SDS PAGE of whole cell lysate was resolved by Coomassie Blue-staining. M, protein marker; lane 1, the total proteins of *E. coli* NovaBlue (DE3) [pET-UGD]; lane 2, the soluble fraction of sample 1; lane 3, the total proteins of *E. coli* NovaBlue (DE3) [pET-ORF1]; lane 4, the soluble fraction of sample3; lane 5, the total proteins of *E. coli* NovaBlue (DE3) [pET100-ORF3]; lane 6, the soluble fraction of sample5; lane 7, the total proteins of *E. coli* NovaBlue (DE3) [pET-ORF15]; lane 8, the soluble fraction of sample 7. Arrows represent the recombinant proteins.

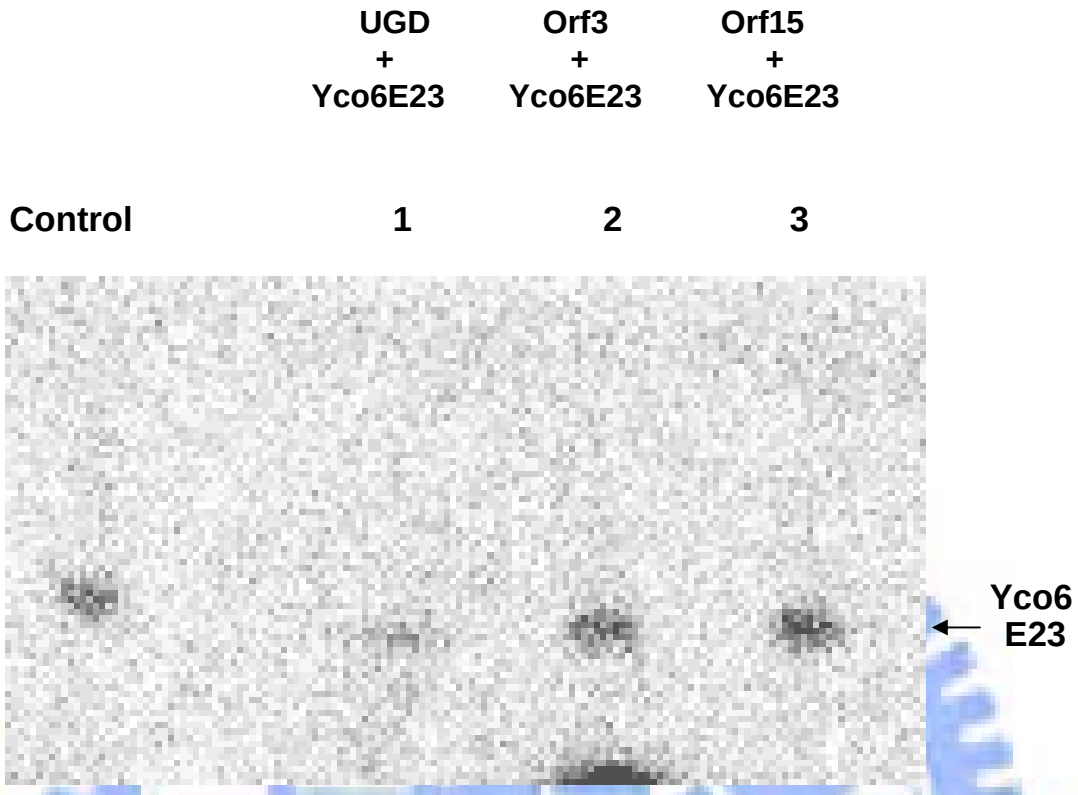

Fig. 17. In vitro phosphorylation assay. Yco6E23 was incubated with Ugd, Orf3 and Orf15 respectively in reaction buffer containing [γ-P^{32}] ATP as substrates at 37 ℃ for 30 min. The reaction mixture was then separated by 12.5% SDS-PAGE. Control, Yco6E23；lane 1, Ugd and Yco6E23；lane 2, Orf3 and Yco6E23；lane 3, Orf15 and Yco6E23.

Apendix 1

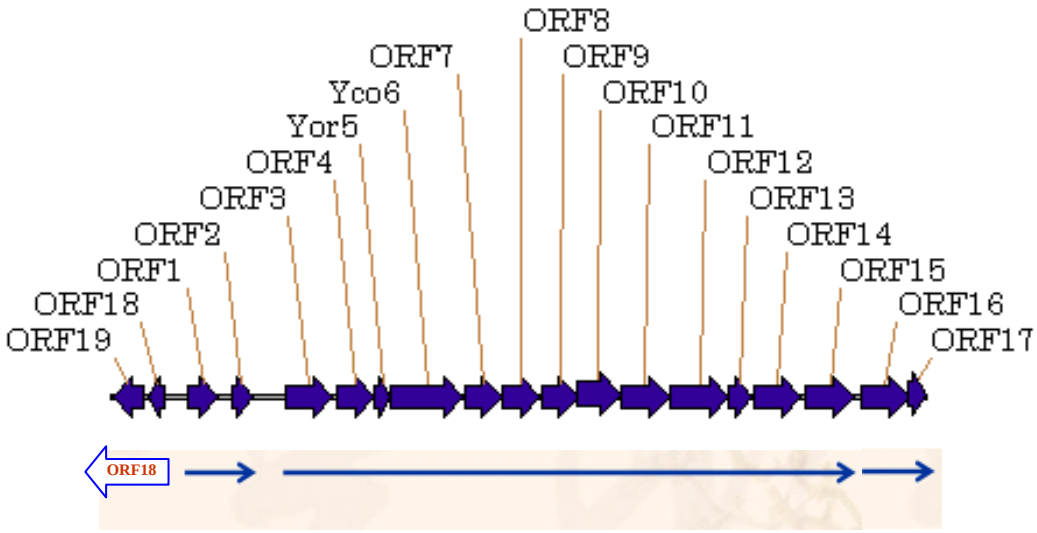

J Bacteriol. 1995 Apr;177(7):1788-96

Organization of the *K. pneumoniae* K2 *cps* gene cluster. Physical map of the chromosomal 20-kb region carrying the *K. pneumoniae cps* gene cluster is shown. The horizontal arrows below represent the putative transcriptional units. The white arrow represents the gene (ORF18) of *K. pneumoniae* NTUH-K2044.

Apendix 2

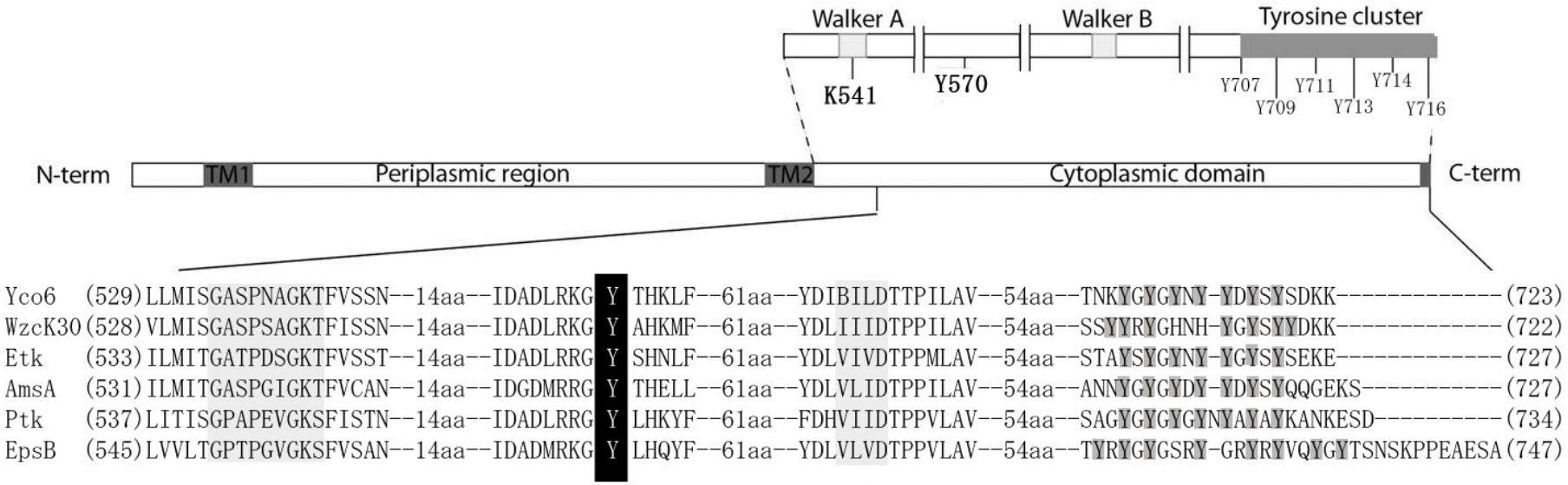

Sequence alignment and structural features of several PTKs. The PTK cytoplasmic domain of Yco6 from *K. pneumoniae* K2 is presented in the *middle section*. The Walker A and B ATP-binding motifs are indicated as *light gray shaded boxes*. The Lys^{541} residue of Walker A, the intraphosphorylated Tyr^{570} residue, and the tyrosine residues of the tyrosine cluster (Tyr^{707}, Tyr^{709}, Tyr^{711}, Tyr^{713}, Tyr^{714} and Tyr^{716}) are indicated with one-letter code (*Y707, Y709, Y711, Y713, Y714* and *Y716* respectively).The two predicted transmembrane α-helices of the PTKs termed TM1 and TM2, are indicated by *dark shaded boxes*. The C-terminal cytosolic PTK domain is enlarged, and sequence alignment of PTKs from Gram-negative bacteria (*Klebsiella pneumoniae* Yco6, *E. coli* K30 Wzc, *E. coli* E2348/69 Etk, *Erwinia amylovora* AmsA, *Acinetobacter johnsonii* Ptk, and *Rastonia solanacearum* EpsB) by using the Vector NTI program. *Dashes* indicate gaps introduced in the alignment process. Tyrosine residues of the tyrosine cluster and the Walker A and Walker B ATP-binding motifs are in *gray boxes*. Catalytic lysine of the Walker A motif is *boldfaced*. Tyr-569 is in a *black box*.